GROUND-WATER FLOW AND STREAM-AQUIFER RELATIONS IN THE NORTHERN COASTAL PLAIN OF GEORGIA AND ADJACENT PARTS OF ALABAMA AND SOUTH CAROLINA

By Robert E. Faye and Gregory C. Mayer

U.S. GEOLOGICAL SURVEY

Water-Resources Investigations Report 88-4143

Atlanta, Georgia

1990

DEPARTMENT OF THE INTERIOR

MANUEL LUJAN, JR., Secretary

U.S. GEOLOGICAL SURVEY

Dallas L. Peck, Director

For additional information
write to:

U.S. Geological Survey
Southeastern Region
R.B. Russell Federal Building
75 Spring Street, S.W., Suite 772
Atlanta, Georgia 30303
(Telephone: (404) 331-5174))

Copies of this report can be
purchased from:

U.S. Geological Survey
Books and Open-File Reports Section
Federal Center, Box 25425
Denver, Colorado 80225

CONTENTS

ILLUSTRATIONS

TABLES

TABLES--continued

PLATES
(In Pocket)

CONVERSION FACTORS

For use of readers who prefer to use metric (International System) units, conversion factors for inch-pound units used in this report are listed below:

Multiply inch-pound unit	By	To obtain metric unit
foot (ft)	0.3048	meter (m)
foot per day (ft/d)	0.3048	meter per day (m/d)
foot squared per day (ft^2/d)	0.0929	meter squared per day (m^2/d)
foot squared per second (ft^2/s)	0.0930	meter squared per second (m^2/s)
cubic foot per second (ft^3/s)	0.02832	cubic meter per second (m^3/s)
cubic foot per second per square mile [$(ft^3/s)/mi^2$]	0.01093	cubic meter per second per square kilometer [$(m^3/s)/km^2$]
inch (in.)	25.40	millimeter (mm)
inch per year (in/yr)	25.40	millimeter per year (mm/yr)
mile (mi)	1.609	kilometer (km)
square mile (mi^2)	2.590	square kilometer (km^2)

****

Sea level: In this report "sea level" refers to the National Geodetic Vertical Datum of 1929 (NGVD of 1929)--a geodetic datum derived from a general adjustment of the first-order level nets of both the United States and Canada, formerly called "Mean Sea Level of 1929."

GROUND-WATER FLOW AND STREAM-AQUIFER RELATIONS IN THE NORTHERN COASTAL PLAIN OF GEORGIA AND ADJACENT PARTS OF ALABAMA AND SOUTH CAROLINA

By Robert E. Faye and Gregory C. Mayer

ABSTRACT

Digital cross-section models, hydrograph separation, and other analytical methods were used to describe ground-water flow and stream-aquifer relations for the clastic Coastal Plain aquifers of eastern Alabama, Georgia, and western South Carolina. Cross-section model simulations indicate that the spatial distribution of net recharge and discharge is highly variable and ranges from less than 1.0 to about 20 inches per year. The water-table configuration largely determines the distribution of hydraulic potential in cross section at least to the top of the uppermost regional confining unit. Simulated discharge to the largest rivers ranges from about 7 to 17 percent of total net recharge and represents flow along the longest flowpaths of a cross section.

A hydrologic budget indicates that total mean annual aquifer recharge equals about 9,000 cubic feet per second. Of this quantity, 780 cubic feet per second is discharged from the regional flow regime to regional drains, 1,950 cubic feet per second is discharged from the intermediate flow regime to streams tributary to regional drains, and 5,150 cubic feet per second is discharged from the local flow regime to streams near the point of recharge. Evapotranspiration occurs at a rate of 660 cubic feet per second. A subsurface flow of 310 cubic feet per second occurs downgradient from the study area and represents that component of recharge not discharged to any stream.

INTRODUCTION

Studies of the major aquifer systems in the United States by the U.S. Geological Survey are a part of the Regional Aquifer Systems Analysis (RASA) Program. A major objective of the RASA Program is the assembly of quantitative hydrologic information that can be used to effectively manage the Nation's ground-water resources (Bennett, 1979). The Southeastern Coastal Plain RASA describes and quantifies flow in major clastic Coastal Plain aquifers between Mississippi and North Carolina (Miller and Renken, 1988) and is divided into subregional project areas to facilitate detailed investigations. The Georgia Subregion, which is the focus of this study, includes about 60,000 square miles (mi^2) of Georgia and adjacent parts of Alabama and South Carolina (fig. 1).

An integral part of the Georgia Subregion RASA is the calibration of a digital computer model which simulates areal ground-water flow within a multilayer aquifer system (fig. 1).

The areal extent of hydrologic investigations described in this report corresponds to the northern one-half to one-third of the Georgia Subregion (fig. 1). Accordingly, the study area is bounded to the north by the Inner Margin of Coastal Plain sediments, to the south by the approximate boundary between clastic and carbonate rocks, and to the east and west by respective drainage divides of the Savannah and Chattahoochee Rivers (pl. 1). The northern, western, and eastern boundaries of the study area also correspond to boundaries or partial boundaries of the Georgia Subregion areal flow model.

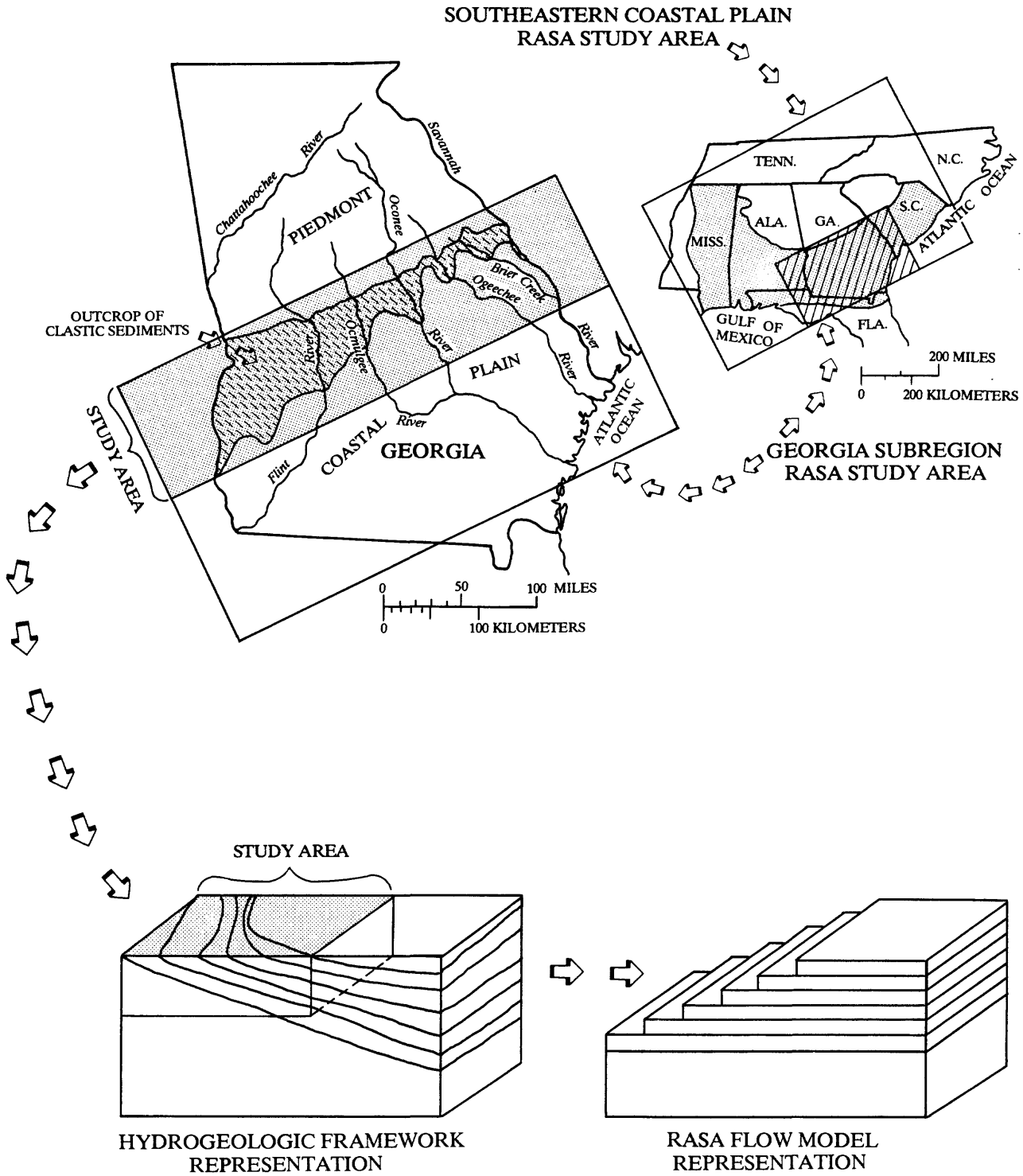

Figure 1.--Location of study area, relation to Southeastern Coastal Plain Regional Aquifer Systems Analysis (RASA) and Georgia Subregion, and schematic representation of the RASA flow model.

The Inner Margin of Coastal Plain sediments marks the geologic boundary between unconsolidated Coastal Plain sediments and consolidated Piedmont rocks. Piedmont rocks also underlie Coastal Plain sediments throughout most of the study area.

Hydrologic and Hydrogeologic Settings

Coastal Plain clastic sediments comprise a seaward thickening wedge of generally unconsolidated units that range in age from the Late Cretaceous to early Tertiary (Miller and Renken, 1988). In general, successively younger sediments crop out seaward of and overlie older sediments. Deposition of these sediments occurred within a variety of environments generally classified as fluvio-deltaic. As such, Coastal Plain sediments are comprised largely of sand and interbedded or lensoidal deposits of clay. The areal extent and thickness of most of the clays are relatively small near the Inner Coastal Plain Margin and distribution is considered to be local. The thickness and areal extent of laterally continuous deposits of sand and clay progressively increase seaward of outcrop areas and the sediment column can be subdivided into major subregional aquifers and confining units (Renken, 1984). The thickness of Coastal Plain sediments near the southern periphery of the study area may exceed 1,500 ft.

The ground-water flow systems of the Georgia Subregion originate in outcrop areas generally near and somewhat south of the Inner Coastal Plain Margin (fig. 1) where precipitation recharges the clastic subregional aquifers. Within this recharge area, subregional aquifers discharge to evapotranspiration and to nearby rivers and streams that dissect the aquifers. Potentiometric maps by Faye and Prowell (1982), Clarke and others (1983, 1984, 1985), and Brooks and others (1985) indicate that stream-aquifer relations and topography in the recharge areas appear to largely control the distribution and patterns of ground-water flow. South of the recharge area, the subregional aquifers become increasingly confined and are progressively buried deeper in the subsurface. Discharge from confined aquifers in downgradient parts of the Subregion is primarily as upward leakage to adjacent aquifers.

Hydraulic characteristics of aquifers within the study area are described by Faye and McFadden (1986). Reported transmissivities of clastic subregional aquifers range from less than 500 to about 40,000 square feet per day (ft^2/d). Storativity ranges from about magnitude 10^{-3} to 10^{-5} and most values are of magnitude 10^{-4}.

Although data relative to clastic sediment anisotropy are few, laboratory analyses (Core Laboratories, Inc., written commun., Aug 13, 1980; Christl, 1964; Marine, 1979) suggest that horizontal conductivities may exceed vertical conductivities by several orders of magnitude.

Precipitation in the Georgia Subregion occurs almost entirely as rainfall and ranges from about 44 to 50 inches per year (in/yr) (Carter and Stiles, 1983; Bingham, 1982; and United States Study Commission-Southeast River Basins, 1973). Areal variation of mean annual rainfall is shown on plate 2. Annual precipitation generally increases from north to south across the Subregion and decreases from the eastern and western peripheries of the Subregion toward the east-central Coastal Plain of Georgia.

The highest order streams that drain the Georgia Subregion are herein referred to as regional drains and all head north of the Subregion in the

Piedmont or Blue Ridge physiographic provinces (fig. 1). The Chattahoochee River is the westernmost regional drain and forms much of the Georgia-Alabama State line. The Flint River drains to the south and southwest across the western Coastal Plain of Georgia and joins the Chattahoochee River near the Georgia-Florida State line. The combined rivers form the Apalachicola River, which flows south across the Florida Panhandle to the Gulf of Mexico. The Ocmulgee and Oconee Rivers flow to the southeast and join to form the Altamaha River in south-central Georgia. The Altamaha River flows eastward and southeastward to discharge to the Atlantic Ocean in the vicinity of Brunswick, Ga. The Ogeechee River heads just north of the Coastal Plain Margin in eastern Georgia and flows generally southeastward across the Coastal Plain to discharge to the Atlantic Ocean. The Savannah River is the easternmost regional drain and forms most of the Georgia-South Carolina State line. The Savannah River also flows to the southeast and discharges to the Atlantic Ocean near Savannah, Ga. Brier Creek, a major tributary to the Savannah River, heads in the Piedmont physiographic province just north of the Coastal Plain Margin in Warren County, Ga., and drains a large area of east-central Georgia before joining the Savannah River near Sylvania, Ga., in Screven County (pl. 1).

Annual runoff in the Georgia Subregion is highly variable and ranges from about 0.8 to 1.7 cubic feet per second per square mile [$(ft^3/s)/mi^2$] (Carter and Stiles, 1983) (pl. 3). Runoff appears to be most variable in the southwestern part of the Subregion where seaward increases in runoff may be the result of hurricane-generated precipitation in coastal areas. Runoff also appears to be uniquely high in southwest Georgia between Sumter County and the Inner Coastal Plain Margin and in central Georgia in the vicinity of Dodge County. Runoff seems to be anomalously low near the Chattahoochee River in the vicinity of Bullock County, Ala., and Stewart County, Ga.

Description of the Problem

At the beginning of Georgia Subregion RASA investigations, most of the hydrologic information necessary to accurately calibrate a subregional flow model was unavailable. Although continuous records that included periods of low streamflows and drought flows, as well as results of seepage investigations, were available at a number of sites, annual baseflow rates required for model calibration were not available in most of the study area. Potentiometric data also were available but were severely limited in quantity and areal distribution. Fewer than 5 percent of the active subregional areal flow model cells corresponded to locations of observed ground-water levels, and these were limited largely to the northern half of the Coastal Plain. Additionally, site data describing the vertical distribution of head within the various subregional aquifers were available at only a few locations. Virtually no data describing recharge rates or the spatial distribution of recharge were available. Data that could be used to describe aquifer hydraulic characteristics were limited to several dozen sites within the northern part of the Coastal Plain (Faye and McFadden, 1986) and were insufficient to determine large-scale trends or distributions useful for subregional flow model calibration.

Major prospective no-flow boundaries of the Georgia Subregion areal flow model included the contact between clastic and Piedmont rocks at the Inner Margin and base of Coastal Plain sediments and potentiometric divides that were considered generally coincident with the drainage divides of the Chattahoochee River to the west and the Savannah River to the east (pl. 1). Whether or not

these topographic and geologic boundaries corresponded to effective hydraulic boundaries for the subregional flow model had not been determined prior to RASA investigations.

Given the paucity and poor distribution of available hydrologic data, a unifying concept that could explain ground-water flow and stream-aquifer relations at a subregional scale was a practical necessity for reliable flow model calibration. Although various reports describing investigations of areally extensive aquifers within the Georgia Subregion were available (Brooks and others, 1985; Clarke and others, 1983, 1984, 1985; Faye and Prowell, 1982), a conceptual model relating local hydrologic observations and descriptions to a general continuum of subregional ground-water flow had not been developed. Furthermore, potentially useful theoretical concepts of large-scale, areally extensive ground-water flow developed and applied elsewhere (Toth, 1962, 1963; Freeze, 1966; Winter, 1976) had not been tested or evaluated with respect to aquifer systems within the southeastern Coastal Plain.

Hydrograph separation methodologies had been used to compute annual rates of baseflow to streams within and near the margins of the Georgia Subregion (Daniel, 1976; Stricker, 1983). Prior to RASA investigations however, the validity and usefulness of these methods had not been evaluated for major rivers of the southeastern Coastal Plain nor had reported baseflows been related to the mean annual rates necessary for flow model calibration.

Purpose of Study

A principal purpose of the Georgia Subregion RASA was the calibration of a multilayer, digital model describing large-scale ground-water flow (fig. 1). Because of the lack of pertinent hydrologic information, a reasonable model calibration was not initially possible. Accordingly, a variety of analytical techniques were used to estimate hydrologic and hydraulic data and to test basic assumptions and concepts applied to RASA model construction and calibration.

The purpose of this report is not to discuss the calibration of the RASA flow model but, rather, to document the results of the independent hydrologic interpretations and analyses used to support flow model calibration. Specific components of this study included:

1. Development of two-dimensional, cross-section flow models to test and evaluate a conceputal model of ground-water flow and stream-aquifer relations;

2. development of a ground-water budget based on estimates of mean annual baseflow at regional drains. Major components of the budget are mean annual rates of aquifer recharge, baseflow, evapotranspiration, and downgradient subsurface discharge;

3. use of analytical methods to evaluate and test assumptions regarding subsurface flow to or out of the study area at the Inner Margin of Coastal Plain sediments and transverse to the eastern and western boundaries of the study area;

4. determination of the diffusivity and related transmissivity for areally extensive aquifers contributing to major Coastal Plain rivers and evaluating corresponding spatial trends and distributions; and

5. demonstrating the application of a selected hydrograph separation methodology to the analysis of major river discharge data. The hydrograph separation method used in this study is herein termed the Rorabaugh-Daniel method (Rorabaugh 1960, 1964; Daniel, 1976).

Methods and Approach

A conceptual model that describes the distribution and patterns of ground-water flow in the study area was developed based on results of previous investigations by Toth (1962, 1963), Freeze (1966), Freeze and Witherspoon (1966, 1967), and Winter (1976). These studies suggested that flow within areally extensive aquifer systems could be subdivided into local, intermediate, and regional flow regimes and that discharge from the regional flow regime is exclusively to regional drains along relatively long flowpaths. By definition, total aquifer discharge to streams or total baseflow from a designated drainage can be accounted for only at regional drains. The term regional flow or regional flow components as used henceforth in this report conforms to the definition of Toth (1962, 1963) and does not imply or describe ground-water flow that may traverse the Georgia Subregion downgradient of the study area defined in this report (fig. 1).

The conceptual model of ground-water flow was tested and evaluated in part by the calibration of two digital cross-section ground-water flow models, similar to those described by Freeze (1966). These cross-section models apply only to discrete flow lines within the northern part of the Georgia Subregion and are not to be confused with the Georgia Subregion areal flow model.

A ground-water budget for the Georgia Subregion was developed and based on computations of mean annual baseflow, evapotranspiration, downgradient subsurface discharge, subsurface flow across the Inner Margin of Coastal Plain sediments, and subsurface flow at the eastern and western boundaries of the study area. Because steady-state, chiefly predevelopment flow conditions prevailed throughout most of the study area during the period of data collection, total aquifer recharge was considered equal to total aquifer discharge.

Annual streamflow data were separated into components of aquifer discharge and surface runoff using the Rorabaugh-Daniel method of hydrograph separation. Gaging station sites were selected to include drainage from all or most of the recharge areas of the clastic subregional aquifers. Evapotranspiration from the water table within the corresponding upstream drainages of these stations was computed as a part of the hydrograph separation analysis. Subsurface recharge from Piedmont rocks across the Inner Margin of Coastal Plain sediments was estimated by using a variant of Darcy's Law. Subsurface discharge from the study area to downgradient parts of the subregional aquifers was computed similarly by using data from Callahan (1964) and represents recharge not discharged to any stream within the study area. The validity of no-flow boundary conditions at major drainage divides was tested at selected locations by estimating the rate of change of potentiometric gradient parallel and normal

to the general topographic line between regional drains. Computed subsurface flow across the Inner Margin of Coastal Plain sediments and at the eastern and western boundaries of the study area proved to be small compared to other budget components. Accordingly, total recharge was computed as the sum of annual baseflow, evapotranspiration, and downgradient subsurface discharge.

Annual baseflow was further subdivided into components of local, intermediate, and regional flow. Regional and intermediate flows were computed by using mass-balance analyses between selected regional drain gaging stations in conjunction with drought streamflow and seepage run data (Thompson and Carter, 1955). Because of the scale and resolution of the subregional areal flow model, the regional component of ground-water flow was of primary interest to this study.

Streamflow recession constants computed as part of the Rorabaugh-Daniel hydrograph separation method were directly related to aquifer diffusivity (Johnston, 1976). Storativity throughout the study area is more uniform than is transmissivity (Faye and McFadden, 1986). Accordingly, the recession constant at each regional drain gaging station was used to measure the combined transmissivity of aquifers that drain to the gage. Furthermore, changes in recession constants from gage to gage were considered a measure of the large-scale, spatial variability of aquifer transmissivity.

The terms "net recharge" and "net discharge" are used in this report to describe the cumulative effect of the several processes of aquifer recharge to and discharge from the water table that may occur simultaneously or during a specified time interval at a particular site or area.

GROUND-WATER FLOW AND STREAM-AQUIFER RELATIONS

Previous quantitative investigations of areally extensive aquifer systems have been based on analyses of ground-water flow in cross section. Hubbert (1940) described steady-state potential and flow directions within a symmetrical cross section of isotropic, homogeneous, porous media designed to represent a lateral series of topographic highs and streams valleys (fig. 2). Characteristic of Hubbert's potential distribution was a boundary beneath each divide and valley beyond which no lateral flow could occur. The regional aquifer system was thus shown to be potentially divisible into a lateral series of adjacent independent regional subsystems, each bounded by a paired divide and valley and each containing the entire flowpaths of all water recharged to and discharged from the subsystem. The shaded area PQRS in figure 2 schematically portrays a regional subsystem. Hubbert's analysis presumed that aquifer thickness was significantly greater than total subsystem relief.

Toth (1962, 1963) extended Hubbert's work to the cross-sectional analysis of large-scale ground-water flow. He recognized that the distribution of ground-water potential within a regional subsystem (fig. 2) could be computed by solving Laplace's equation constrained by impermeable boundaries at the base and sides of the subsystem (PQ, QR, and RS in fig. 2) and by a water-table condition at the top (PS in fig. 2). The water table in Toth's analyses increased linearly or sinusoidally between the stream valley and the divide. The locations of vertical zero-flow boundaries at the sides of the subsystem were considered to be controlled by the locations of the major topographic divide and the major valley drain. The basal impermeable boundary was horizontal. The

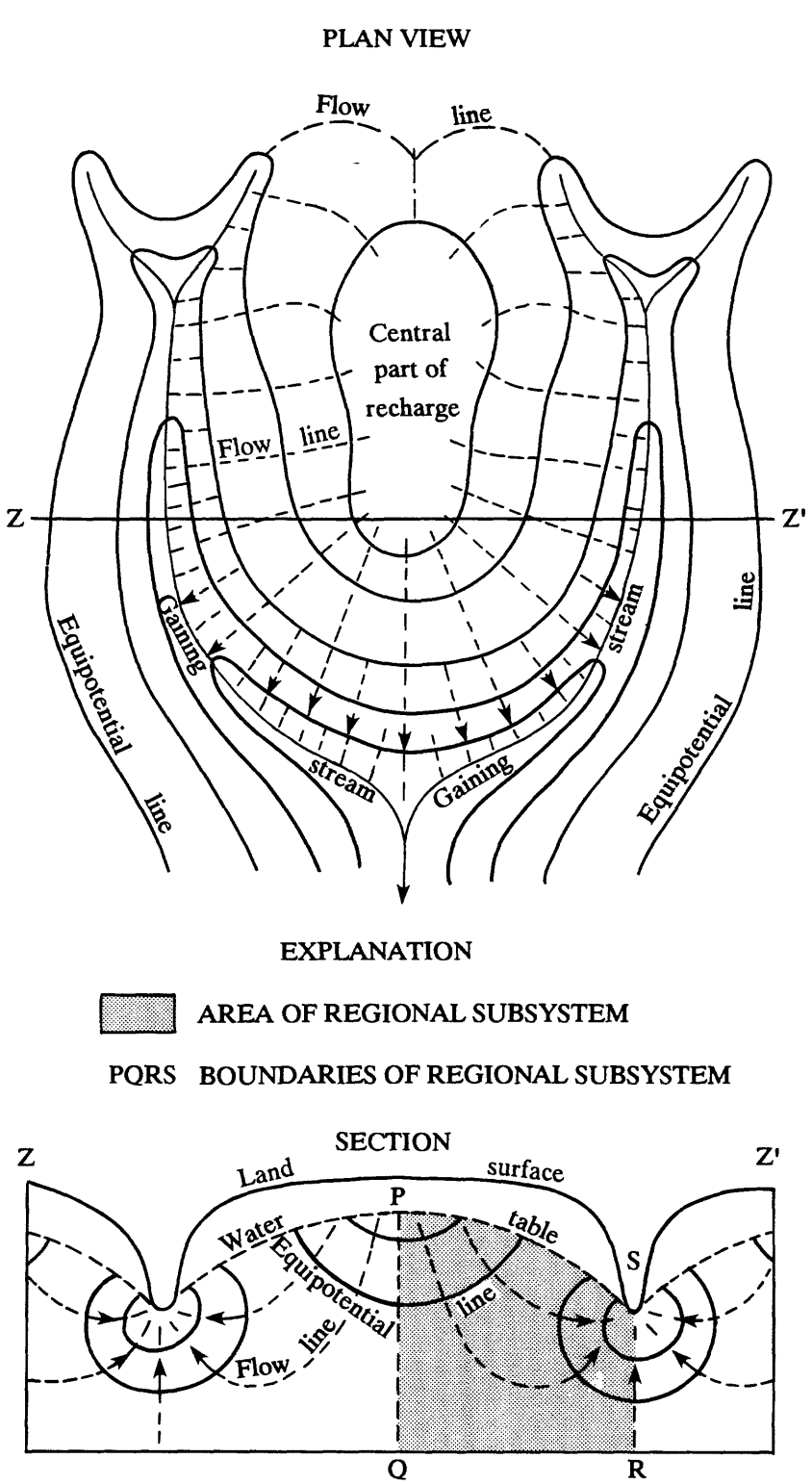

Figure 2.--Lateral and vertical distribution of ground-water flow and potential within an areally extensive, isotropic, homogeneous aquifer system. Modified from Hubbert, 1940 and Heath, 1983

water table was considered to be in steady state; that is, stationary with time. This condition is not precisely true but is considered valid if real water-table fluctuations are small with respect to total aquifer thickness and if the relative configuration of the water table is maintained through the cycle of fluctuations. Where such conditions are satisfied, the water table is in a state of dynamic equilibrium (Freeze and Witherspoon, 1966) and water-table heads represent their long-term average potential. A condition of dynamic equilibrium also suggests that average annual precipitation is sufficient to maintain a completely recharged aquifer system on a long-term basis. Toth's analysis also required the aquifer system to be isotropic, homogeneous, and unconfined. Implicit in Toth's work is the assumption that topographic highlands are areas of net ground-water recharge, whereas corresponding lowlands are areas of net discharge.

Toth (1963) observed that most ground-water-flow systems could be qualitatively subdivided into paths of local, intermediate, and regional flow, depending on the thickness and lateral extent of the subsystem and the degree of local topographic relief. A local flowpath was defined as a relatively shallow path extending from a recharge (highland) area to an adjacent discharge (lowland) area. Intermediate flowpaths include at least one local flow system between their respective points of recharge and discharge and are somewhat deeper and longer than local paths. Regional flowpaths begin at the major subsystem divide and continuously traverse the entire regional subsystem to the major drain. Regional flowpaths are the longest and deepest of the regional subsystem. Toth (1963) further states that net recharge and, consequently, ground-water flow are distributed according to local, intermediate, or regional flow regimes, with flow and net recharge being greatest within local systems and least within regional systems. Additionally, Toth (1963) considered the effects of climatic variation to be greatest within local flow systems and least within regional systems. Several illustrations representative of Toth's analyses are shown in figure 3.

Freeze (1966) and Freeze and Witherspoon (1966, 1967) extended Toth's concepts to the general case using a numerical model. Numerical model analyses facilitate the investigation of cross-sectional ground-water flow systems characterized by irregular water-table configurations and varying degrees of aquifer anisotropy and heterogeneity. A large number of theoretical cross-sectional flow systems were studied using a variety of water-table configurations and aquifer hydraulic conductivity distributions (Freeze, 1966; Freeze and Witherspoon, 1967). Assumptions regarding the impermeable basal and lateral boundaries, steady-state flow, and a water table in dynamic equilibrium established by Toth were maintained. Although largely theoretical, these model studies further enlarged upon several of the concepts of areally extensive ground-water systems first identified by Toth (1962, 1963). Of particular importance to the Georgia Subregion were studies of topographic irregularities and their corresponding replication by the water-table. Major valleys were shown by Freeze and Witherspoon (1966, 1967) to be areas of concentrated net ground-water discharge, whereas net recharge was shown to be concentrated at major water-table (topographic) highs and at the regional subsystem divide. The occurrence of numerous irregularities in the water-table configuration was shown to create a corresponding number of local flow systems superposed on a single regional flow system, causing complex potential and recharge-discharge distributions.

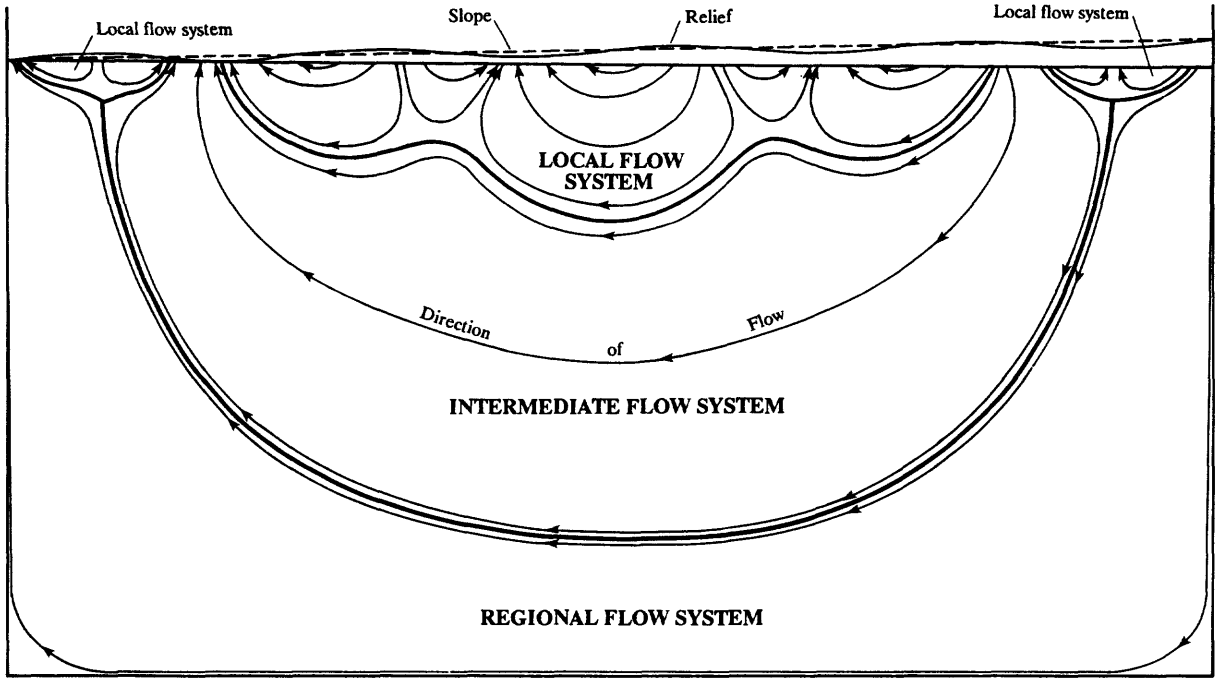

Modified from Toth (1963)

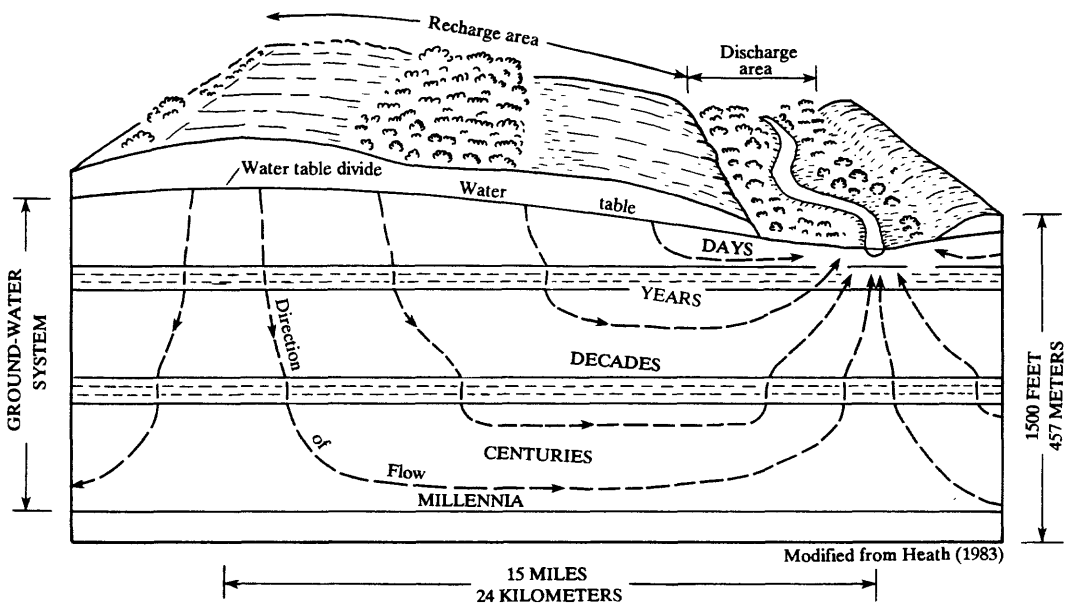

Modified from Heath (1983)

Figure 3.--Examples of local, intermediate, and regional ground-water flow.

Hitchon (1969) applied Toth's concepts to the investigation of regional fluid potential and flow within an areally extensive group of clastic (?) formations in western Canada. Using a large number of drill-stem-test and bottom-hole-pressure data, he constructed a number of potentiometric surface maps showing fluid potential at given depth intervals relative to sea-level datum. The thickness of a sediment "slice" represented by each map ranged from 250 to 1,000 ft, depending on the density of data. These maps and a number of cross sections showing fluid potential were used to investigate the correlation of regional topography with fluid flow. Hitchon determined that despite regional differences in geology, major and minor regional topographic features markedly influenced the distribution of fluid potential and flow at depth and exerted a major control on the occurrence of recharge and discharge and local flow systems. Drawdown effects at regional drains were observed to depths of 5,000 ft.

Conceptual Model

A conceptual model of ground-water flow within the study area probably applies equally well to most of the northern Coastal Plain between the Cape Fear Arch and the Mississippi River Embayment (not labeled in area of fig. 1). Characteristics of the conceptual model are based on previous investigations and analyses of areally extensive ground-water flow. The complexity of Coastal Plain hydrology and geology is such that all elements of the conceptual model may not be represented everywhere. Major elements of the conceptual model include flow regimes, net recharge and discharge, aquifer anisotropy, stream-ground-water relations, and fluid potential. All remarks pertain to a regional subsystem.

Flow Regimes

Throughout most of the study area, sediment thickness is considerably larger than total watershed relief and the regional subsystem can be subdivided into local, intermediate, and regional ground-water-flow regimes. Local flow regimes are characterized by relatively shallow and short flowpaths that extend from a topographic high to an adjacent topographic low. Intermediate flowpaths are longer and somewhat deeper than local flowpaths and intermediate flow regimes contain at least one local flow system. Regional flowpaths begin at or near the major subsystem divide and terminate at the regional drain. Regional flowpaths are the deepest flowpaths of the regional subsystem. The number, distribution, and depth of influence of local flow regimes are largely a function of water-table configuration and aquifer thickness relative to watershed relief. Near the Inner Coastal Plain Margin where aquifer sediments are thin compared to topographic relief, local flow regimes may predominate and intermediate and regional flow regimes may not occur. Boundaries between flow regimes, which can be theoretically determined, can only be qualitatively described in practice. Because of the relative location of flow regimes, shallow to deep, within a vertical section, the effects of climatic variability are most pronounced on local flow regimes and least pronounced on regional flow regimes.

Net Recharge and Discharge

The distribution of net recharge and net discharge is sufficiently influenced by the water-table configuration such that net recharge occurs in

highland areas and net discharge occurs in lowland areas. Quantities of net recharge and net discharge are variably distributed throughout the local, intermediate, and regional flow regimes and are greatest for local regimes and least for regional regimes. Ground-water discharge to the regional drain occurs largely from the regional flow regime. Discharge to streams tributary to the regional drain is almost entirely from local and intermediate flow regimes. Net recharge to regional flow regimes occurs largely near the major subsystem divide. Net recharge to intermediate and local flow regimes occurs along the major divide as well as at other highland areas. A single hinge line may occur which subdivides a regional subsystem into general areas of net recharge and net discharge. Depending on the complexity of and interaction between flow regimes, multiple hinge lines may be present. Where regional drain incisement is great relative to aquifer thickness (such as near the Inner Coastal Plain Margin) the hinge line may occur closer to the drain than to the major subsystem divide. Where drain incisement is small compared to aquifer thickness, the hinge line may occur closer to or at the midpoint of the regional subsystem.

Aquifer Anisotropy

The smaller the difference between vertical and horizontal conductivity within a regional subsystem the more equally distributed are net recharge and discharge among flow regimes. Net discharge to the regional drain and local quantities of net recharge and discharge tend to increase with decreasing anisotropy.

Stream and Ground-Water Relations

Local and intermediate flow regimes discharge ground water largely to streams tributary to the regional drain. In general, the lower the tributary stream order the larger the relative contribution to baseflow from the local flow regime. Discharge from the regional flow regime occurs at the regional drain and perhaps along the downstream reaches of the largest tributary streams. Net discharge to the regional drain is controlled largely by the total relief and length of the regional subsystem, aquifer anisotropy and conductivity, and incisement of the regional drain.

Fluid Potential

The water-table of the regional subsystem approximates a subdued replica of land-surface topography. The depth of influence of the water-table configuration on subsystem fluid potential is limited largely to the local flow regime, but, in the absence of areally extensive confining units, may extend to the intermediate and regional flow regimes as well. Fluid potential in the vicinity of the major divide decreases with depth, probably to near the base of the regional subsystem. Conversely, fluid potential in the vicinity of the regional drain increases with depth.

The influence of topography on ground-water flow and potential has been observed in areally extensive aquifers within the Georgia Subregion. Potentiometric surface maps of the major aquifers of Cretaceous and Tertiary age near the Coastal Plain Margin and the Savannah River in Georgia and South Carolina are shown by Faye and Prowell (1982) and, in modified form, on plates 4 and 5. A large number of data were used to construct each map and the maps include the area of outcrop of each aquifer as well as adjacent areas where

aquifer sediments are buried. The Tertiary aquifer overlies the Cretaceous aquifer and is separated from the Cretaceous aquifer by thick, areally extensive layers of laminated clay and mudstone of Paleocene age. Although potential differences between the aquifers can exceed 100 ft within the seaward half of the Coastal Plain, the potential distributions of each aquifer are uniformally similar and generally symmetrical to the Savannah River, a regional drain. The influence of topography and tributary drains on fluid potential is especially pronounced within and adjacent to outcrop areas.

Increasing fluid potential with depth in the vicinity of regional drains has also been noted throughout the northern part of the Georgia Subregion. Maps published by LaMoreaux (1946), LeGrand and Furcron (1956), and LeGrand (1962) show "area(s) of artesian flow" close to and along the downstream reaches of the Flint, Ocmulgee, Oconee, Ogeechee, and Savannah Rivers. Such areas generally delineate the frequent occurrence of flowing wells where fluid potential at the base of wells exceeds land surface altitude. A specific reference to fluid potential change with depth at a regional drain is reported by Stephenson and Veatch (1915) for a well adjacent to the Flint River at Montezuma, Ga., near the southern periphery of the study area. Fluid potential at this well progressively increased from 8 ft above land surface at a depth of 60 to 62 ft above land surface at a depth of 500 ft.

Similarly, data from several wells proximate to the Savannah River in eastern Burke County, Ga. (Bechtel Corporation, 1973) indicate that heads in a shallow aquifer comprised of lower Tertiary sediments were about 100 ft in altitude in 1973. The altitude of heads in nearby wells in a deeper aquifer comprised of Upper Cretaceous sediments was about 170 ft.

The conceptual model of ground-water flow is based largely on the results of model studies and field investigations that treat regional subsystems similar to, but not entirely characteristic of, regional subsystems within the northern part of the Georgia Subregion. Specifically, regional subsystems within the study area are vertically subdivided into multiple alternating layers of areally extensive aquifers and confining units, whereas most of the theoretical studies by Toth (1962, 1963) and Freeze and Witherspoon (1966, 1967) were based either on unconfined subsystems or subsystems containing a single low-conductivity layer. In addition, the slope of the base of the regional subsystem, which was considered to be horizontal by previous investigators, probably slopes steeply along flow lines within the study area.

Digital Cross-Section Models

A method for corroborating the conceptual model is to duplicate the experiments of Freeze (1966) and Freeze and Witherspoon (1966, 1967) from which the conceptual model was originally derived. Accordingly, two digital cross-section ground-water-flow models of regional subsystems were constructed to represent, as specifically as possible, the hydraulics of major vertically contiguous aquifers within the study area. The line of each cross-section model (pl. 1) was located within the study area according to (1) the availability of geohydrologic, potentiometric, and aquifer-parameter data and (2) the occurrence of spatially coincident flow lines within vertically contiguous, component aquifers. Ground-water flowpaths within component aquifers were inferred from published and unpublished potentiometric maps which generally represent a quasi-predevelopment condition (Faye and Prowell, 1982; Clarke and others, 1983,

1984, 1985; and Brooks and others, 1985). The line shown for each model (pl. 1) is a composite of several flow lines, one from each component aquifer, which are of different lengths but spatially coincident along a common length. Model geometry is based on geohydrologic data at nearby boreholes, the locations of which are shown on plate 1. The models are designated by number as cross-section model 1 or 2.

Methods and Assumptions

Model structure and development

Cross-section models described herein are based on conditions of two-dimensional, steady-state flow within saturated, anisotropic, heterogeneous aquifers. Such conditions can be generally described by the equation:

$$\frac{\partial}{\partial x}\left[K(x,z)\frac{\partial h}{\partial x}\right]+\frac{\partial}{\partial z}\left[K(x,z)\frac{\partial h}{\partial z}\right]=0, \qquad (1)$$

where, x is the coordinate along the flow line in a horizontal plane, in L;

z is the coordinate in a vertical plane, in L;
K is aquifer hydraulic conductivity, in LT^{-1}; and
h is head or fluid potential, in L.

The solution of equation (1) is dependent on the mathematical analogues of the hydraulic conditions that occur at the boundaries of the region of solution. The boundary conditions assumed for cross-section models 1 and 2 conform closely to those of Freeze (1966) such that (1) the base of the subsystem is considered impermeable ($\partial h/\partial z = 0$); (2) flow across the vertical boundaries at the major divide and the regional drain is zero ($\partial h/\partial x = 0$); and (3) the uppermost boundary of the cross-section is represented by the water table which is at steady state ($h = f(x) = \text{constant}$). Pressure distribution along the water table is atmospheric. A schematic representation of a typical cross-section model showing these boundaries and their relation to hydrologic features is shown in figure 4.

The digital model and corresponding numerical methods and solution procedures used in this study are described by McDonald and Harbaugh (1984). In general, the model is based on a finite-difference approximation of equation (1) which is solved using a strongly implicit procedure. A computation of flux across the face of each node and at specified head nodes was determined for each model simulation in order to analyze and compare rates of recharge and discharge and aquifer discharge to streams.

The Cartesian discretization of a typical model is indicated by the nodal cells or rectangles (also called nodes) which uniformally subdivide the solution space (pl. 6; fig. 5). Each cell is designated by a numbered pair (x, z) representing, respectively, the number of the row and column starting at an arbitrary origin (0,0) located at the upper left-hand corner of the grid. Row number is directly proportional to depth. Column number is directly proportional to horizontal distance from the origin. Cross-section miles are measured from the major divide to the regional drain with mile 0.0 at the major divide. The horizontal and vertical dimensions of an individual nodal cell represent, respectively, 2,640 and 50 ft of a regional subsystem. Thus, the

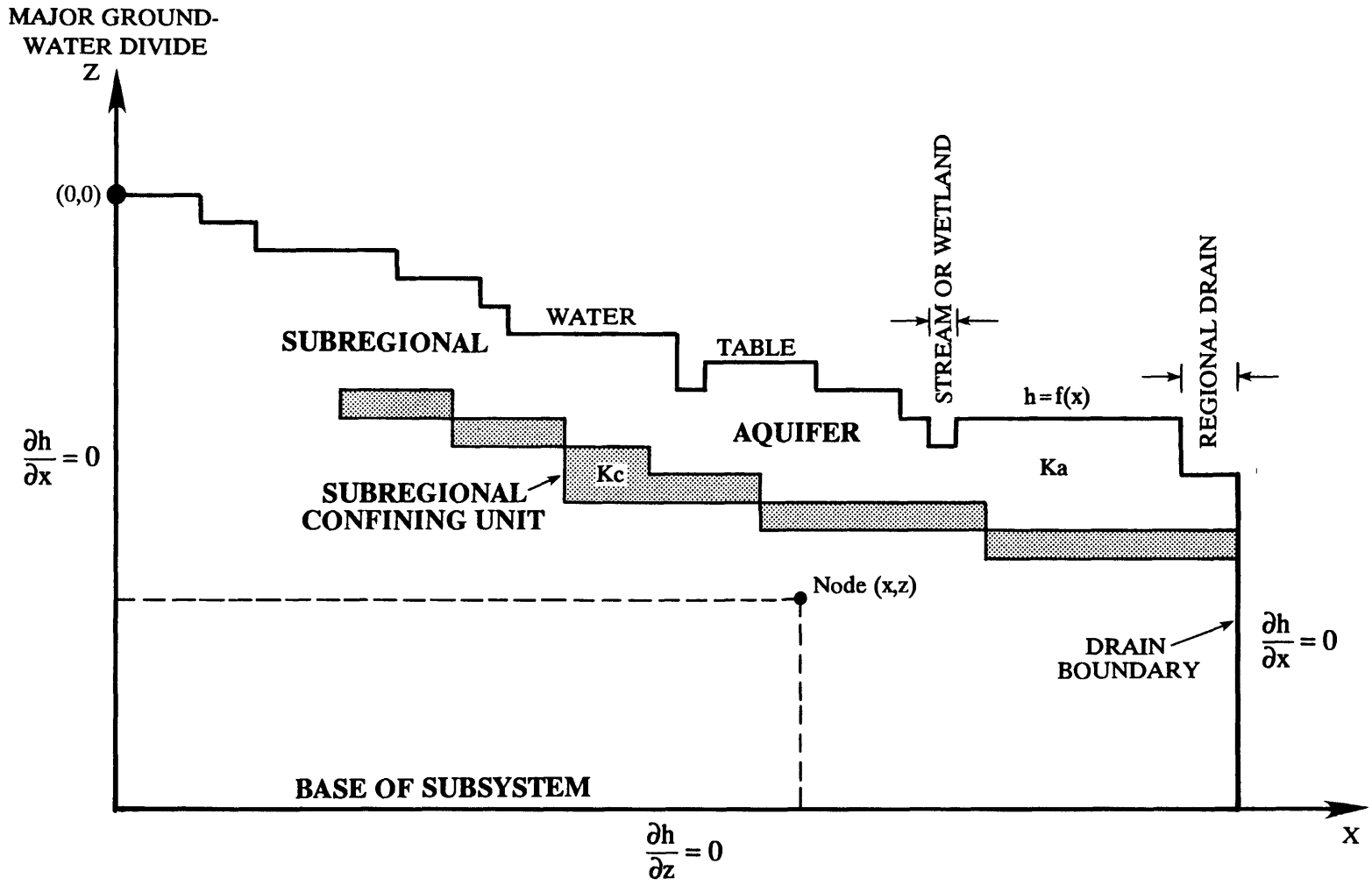

Figure 4.--Schematic representation of boundary conditions and components of a typical cross-section model.

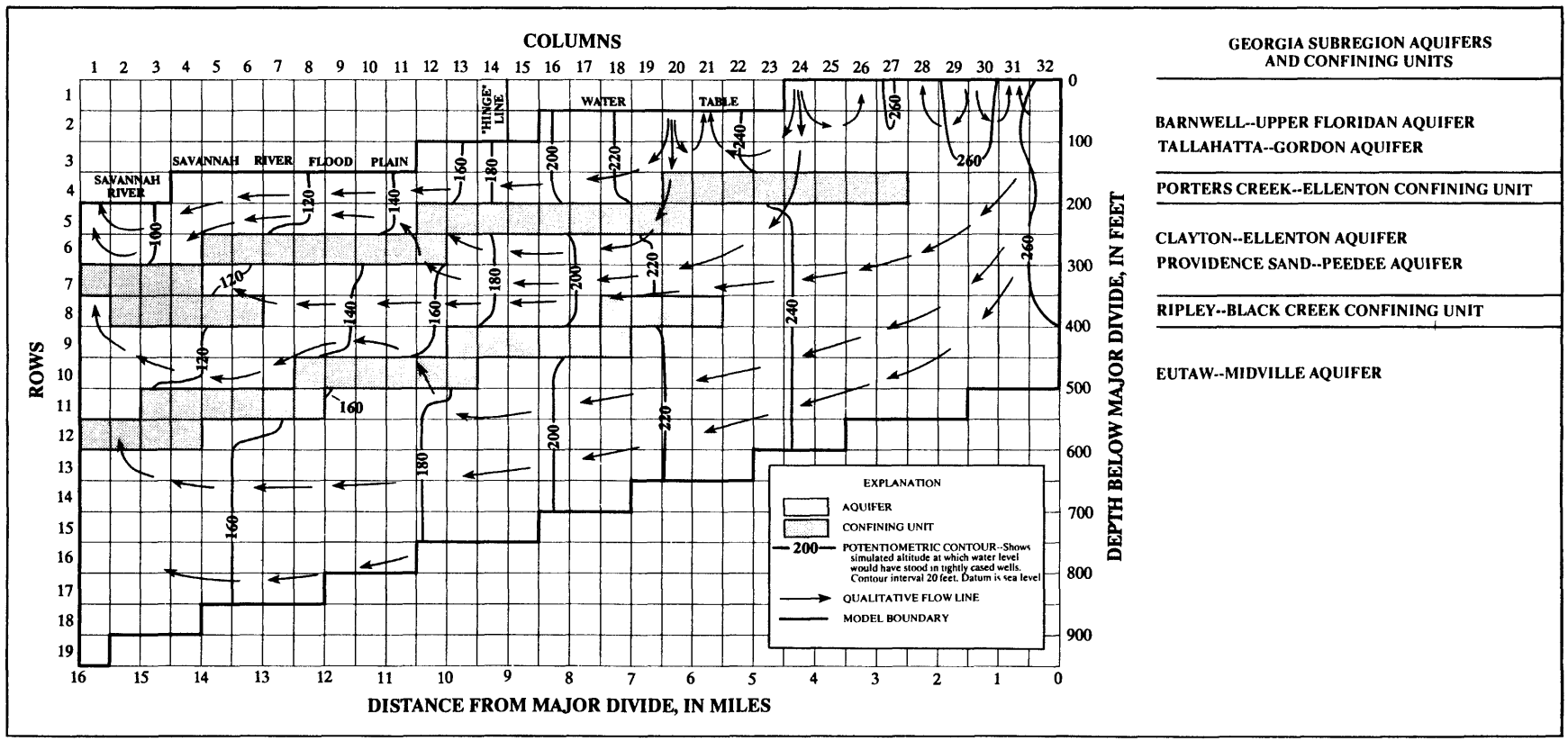

Figure 5.--Model grid, geohydrology, stream-discharge points, and selected flow lines for cross-section model 2.

vertical exaggeration of figures showing ground-water flow and potential (pl. 6; fig. 5) is approximately 53:1. Such exaggeration precludes the presentation of flow diagrams or flow nets that quantitatively represent ground-water flow within a regional subsystem (Van Everdingen, 1963). Note that flow lines which appear highly curved in a vertically exaggerated cross section are actually nearly horizontal.

The subscripted K's, shown in figure 4, indicate hydraulic conductivity values relative to regional aquifers (a) and confining units (c). Lateral hydraulic conductivities of cross-section model aquifers were estimated by dividing computed aquifer transmissivity at nearby wells (pl. 1) by aquifer thickness. Transmissivity estimates were based on time-drawdown or time-recovery aquifer tests (Faye and McFadden, 1986). A few laboratory data describing the hydraulic conductivity of borehole cores were also used (Christl, 1964; Marine, 1979; Cahill, 1982; Clarke and others, 1985). Lateral hydraulic conductivities of confining units were estimated using reported lithologic descriptions and were considered to be one to two orders of magnitude less than corresponding aquifer conductivities.

Anisotropy, the ratio of vertical to horizontal hydraulic conductivity for aquifers and confining units, is not well documented in the study area. Laboratory analyses of conductivities of clastic sediment samples are reported by Christl (1964), Marine (1979), Cahill (1982), and Core Laboratories, Inc. (written commun., 1980) and range from 10^{0} to 10^{-3} in order of magnitude. These analyses are few in number and are pertinent only to the general vicinity of cross-section model 2. A constant single value of anisotropy was applied to each cross-section model and is herein termed model anisotropy.

Boundary conditions and transverse flow

Data deficiencies preclude the absolute verification of the water table and hydraulic boundaries used to delimit the cross-section models (fig. 4). The steady-state water-table boundary represents the condition of dynamic equilibrium and was estimated using water-level data proximate to the cross-section lines and stream altitudes inferred from topographic maps. Where direct measurements of water-table head were unavailable, estimates of head were based on topographic configuration along the cross-section line. The water-table configuration represented by each calibrated cross-section model conforms approximately to the topographic configuration along the line of the cross section. Specified water-table heads act only as sources or sinks for flow computed at underlying nodes. Accordingly, actual flow within the uppermost 50 ft of saturated thickness along the cross-section line is not simulated by the model. Such flow is probably small relative to flow through the total saturated thickness represented by the cross section and is neglected when comparing model results to field conditions.

The validity of no-flow boundaries at the regional drain and major subsystem divide is partly demonstrable with potentiometric data and the interpretation of these data in the form of potentiometric contours. For example, the potentiometric surfaces and related site data in Upper Cretaceous and lower Tertiary sediments south of Augusta, Ga., have been previously shown on plates 4 and 5. The line of cross-section model 2 is also shown. These maps and accompanying potentiometric data indicate that ground-water flow is lateral toward the Savannah River from both the east and west banks. Conversely, flow

appears to be away from a generally southeast trending line parallel to the drainage divide between the Savannah and Edisto Rivers located in central Aiken County, S.C. Accordingly, the imposition of no-flow conditions ($\partial h/\partial x = 0$) at the upstream and downstream boundaries of the cross-section lines seems appropriate.

The base of each cross-section model conforms to the top of consolidated Piedmont rock or the top of a major confining unit. The confining unit is comprised of clay or indurated, cemented clayey sand. The hydraulic conductivity of the consolidated rock or confining unit is probably an order of magnitude or more less than the conductivity in overlying aquifer sands and can be considered relatively impermeable ($\partial h/\partial z = 0$).

The similarity of cross-section model simulations to field conditions is also affected by the occurrence of transverse flow in component aquifers; that is, ground-water flow generally normal toward all or parts of the line of the cross-section model. Transverse flow also may occur at the upstream and downstream boundary points of the cross-section line, parallel to the regional drain or the subsystem divide. If the quantity of transverse flow is large relative to the quantity of flow parallel to the cross-section line, then the assumption of two-dimensional ground-water flow in a vertical plane, as represented by equation 1, may not be valid and cross-sectional flow analyses may be inappropriate.

The flow line of cross-section model 2 is shown on plates 4 and 5 to generally follow a ridge of the potentiometric surfaces. This line also follows potentiometric ridges in overlying component aquifers (potentiometric maps not shown in this report). The flow lines of three of the four component aquifers of cross-section model 1 also follow potentiometric ridges (potentiometric maps not shown in this report). Transverse flow is probably minimal along potentiometric ridges, and ground-water flow normal to or away from intermediate parts of cross-sections 1 and 2 is considered minimal with respect to flow parallel to the cross sections.

Transverse flow at the cross-section model boundaries was estimated by comparing rates of change of head gradient in directions normal and parallel to the cross-section model lines at the respective regional drains and subsystem divides. Although potentiometric data were not available for each component aquifer for each cross-section model, the comparisons made indicated that rates of change of head gradient parallel to the drains and divides were from one-half to two orders of magnitude smaller than corresponding rates of change parallel to the lines. Accordingly, the validity of applying equation (1) to cross-section models 1 and 2 appears not to be significantly compromised by the occurrence of transverse flow either at the boundaries of the cross-section lines or toward intermediate parts of the lines.

These analyses further suggest that essentially no-flow conditions ($\partial y/\partial x = 0$) prevail for most component aquifers at or near the major surface drainage divides within the study area. The western and eastern boundaries of the Georgia Subregion areal flow model generally correspond to major drainage divides within the study area and, accordingly, can be considered no-flow boundaries in the northern part of the Subregion.

Calibration strategy

Calibration of each cross-section model was achieved largely by adjusting the value of model anisotropy and to a much lesser degree the lateral conductivity of confining units and individual specified water-table heads. Calibration was considered satisfactory when (1) observed hydraulic head in wells located near the cross-section line matched computed hydraulic head at the corresponding model nodal cell within 15 ft or less and when (2) computed maximum rates of local net recharge equaled about 20 in/yr.

Computed maximum local rates of net recharge to each cross-section model were estimated to be about 20 in/yr on the basis of average net recharge rates computed by Stricker (1983). Three of the watersheds investigated by Stricker (1983) are within or directly adjacent to areas represented by the cross-section models. Reported net recharge rates at these watersheds range from 11 to 20 in/yr and represent computed baseflow extrapolated over the entire watershed area. Because each of these watersheds contains significant areas of net ground-water discharge, that is areas where the water table is at or near land surface, the maximum local rate of net recharge must be significantly higher than the reported net averages. Thus, the maximum local rate of net recharge of 20 in/yr utilized to calibrate the cross-section models may be somewhat conservative.

Quantities of net discharge to tributary streams and regional drains computed by the cross-section models were compared to observed rates in the general vicinity of the cross-section line. Comparisons of observed baseflows to computed rates of ground-water discharge to streams are not necessarily appropriate for these cross-section models. Observed stream discharge rates are generally based on differences in stream discharge between two points of measurement normalized to a unit stream length (in miles) or to a unit drainage area (in square miles). Only if the given cross section represents quantitatively the average hydrologic conditions within the stream reach which spans the points of stream discharge measurement can a direct comparison be made. There was, of course, no way of designating such a cross section prior to model analysis. Accordingly, if ground-water discharges to streams computed by the cross-section models were within a reasonable range of normalized measured baseflows, the comparisons were considered satisfactory.

Cross-section model computations are based on steady-state conditions with a water table in "dynamic equilibrium." For this study, model computations are additionally considered to represent predevelopment conditions.

Cross-Section Descriptions and Model Results

Cross-section model 1

Cross-section model 1 extends from the major regional subsystem divide between the Flint and Ocmulgee Rivers in Crawford County, Ga., southeast through Peach and Houston Counties to the Ocmulgee River near the common boundary of Houston, Pulaski, and Bleckley Counties (pl. 1). The length of the cross-section path line is about 28 miles as measured on 7 1/2-minute topographic maps. Geohydrologic control was obtained from four boreholes proximate to the cross section that penetrate the entire thickness of Coastal

Plain sediments at cross-section miles 0.0, 5.0, 17.5, and 28.0 (pls. 1 and 6). Data from several intermediate shallower boreholes were also used for geohydrologic control (not shown on pl. 1).

Aquifers and confining units are named using Georgia Subregion RASA nomenclature (Miller and Renken, 1988). In descending order, the component subregional aquifers include the Barnwell-Upper Floridan aquifer, the Tallahatta-Gordon aquifer, the Clayton-Ellenton and the Providence Sand-Peedee aquifers combined, and the Eutaw-Midville aquifer. Similarly, those sediments which correspond to subregional confining units include the Lisbon-McBean confining unit, the Tuscahoma-Fishburne confining unit, and the Ripley-Black Creek confining unit. The base of the cross-section model conforms to the top of the Eutaw-Cape Fear confining unit along most of the section line.

The distribution and thickness of component aquifers and confining units are shown on plate 6. Confining unit thicknesses range from less than 50 ft to more than 150 ft and gradually increase from northwest to southeast. Thickness of the Lisbon-McBean confining unit appears to be more uniform areally than other confining units and generally is less than 50 ft. All extensive confinement seems to "pinch out" toward the northwest. Accordingly, the regional subsystem near the major divide is probably hydraulically equivalent to a single subregional aquifer. Component aquifer thicknesses range from about 50 to 700 ft.

Lateral hydraulic conductivity of aquifer sediments used in the calibrated cross-section model ranges from 2.0 to 20.0 feet per day (ft/d) and was based on computations of transmissivity and aquifer thickness at wells proximate to the cross-section path line at miles 4.5, 14.9, and 21.0. Transmissivity computations at these wells were based on time-drawdown water-level data (Faye and McFadden, 1986). Transmissivity estimates based on specific capacity at several wells were also used to estimate hydraulic conductivities. Aquifer-test and specific-capacity data pertained only to the Tallahatta-Gordon and to the Eutaw-Midville aquifers. Hydraulic conductivities of other units were estimated from lithologic descriptions. Lateral hydraulic conductivity of confining units used in the calibrated model ranges from about 0.2 to 0.6 ft/d. The calibrated model anisotropy ratio is 0.005. Leakance of the model confining units thus ranged from about 10^{-6}/d to about 10^{-5}/d.

Nodally distributed values of lateral hydraulic conductivity used in the calibrated model are shown on plate 7. Corresponding specified water-table heads are listed in table 1. Aquifer conductivity values are shown to generally increase with depth to the Eutaw-Midville aquifer. The lowest aquifer conductivity values (2 ft/d) occur in the vicinity of the water table and near confining units and are characteristic of a clayey sand lithology.

The calibrated model anisotropy of 0.005 is somewhat lower than corresponding anisotropies observed in the Atlantic Coastal Plain (Johnston, 1973, 1977). This model anisotropy, however, may reflect the contrast between aquifer and confining unit vertical hydraulic conductivities rather than the ratio of vertical to horizontal conductivities within individual hydrologic units. The sensitivity of cross-section model results to the contrast in lateral hydraulic conductivity between aquifers and confining units was tested and the results are described as part of the discussion of sensitivity analyses.

Table 1.--Nodally distributed values of water-table head--cross-section model 1

Specified head values, in feet					
Cross-section model one					
Row	Column	Head	Row	Column	Head
1	1	470	3	29	356
1	2	460	4	30	312
2	3	420	5	31	290
1	4	450	4	32	310
2	5	440	4	33	320
2	6	425	5	34	285
2	7	403	4	35	320
3	8	380	5	36	287
3	9	350	5	37	273
3	10	370	5	38	295
3	11	360	5	39	279
4	12	350	5	40	282
3	13	370	5	41	285
3	14	380	5	42	288
4	15	340	4	43	306
4	16	325	4	44	310
4	17	325	4	45	305
3	18	355	4	46	309
3	19	385	5	47	261
3	20	370	5	48	253
3	21	370	5	49	250
3	22	396	5	50	255
3	23	380	6	51	243
3	24	354	6	52	249
3	25	363	5	53	254
3	26	355	6	54	227
4	27	340	6	55	217
4	28	340	6	56	211

The model-computed cross-sectional distribution of hydraulic potential is shown on plate 6 along with selected lines of ground-water flow. These flow lines are strictly qualitative and are meant to indicate only possible flow paths, based on nodally distributed values of computed hydraulic head. Observed hydraulic heads and corresponding computed heads are listed in table 2. Observed head data are not well-distributed throughout the cross section. At the calibrated model anisotropy of 0.005, all computed heads match the observed heads within the 15-foot calibration limit with the exception of the head at nodal cells 14,28 and 10,32. Several of the observed hydraulic heads (nodal cells 16,39; 9,7; and 14,28) were obtained from municipal or industrial wells where pumping of ground-water had occurred over a long period prior to the measurements reported herein. Cross-section model calibration is intended to simulate predevelopment conditions. Consequently, a computed head somewhat greater than the observed head at these nodes is possible. Also, the observed hydraulic head of 296 ft applies to nodal cells 10,39 through 17,39. This head was obtained from a multiaquifer well with a screened interval corresponding to model computed hydraulic heads of 298 and 310 ft.

Table 2.--Sensitivity of computed hydraulic head to changes in model anisotropy--cross-section model 1

[Trpy, model anisotropy]

Node row,	column	Observed hydraulic head (feet)	Computed hydraulic head, in feet				
			Calibrated anisotropy (Trpy = 0.005)	Trpy = 1.0	Trpy = 0.5	Trpy = 0.1	Trpy = 0.05
2,	4	423	438	449	449	447	446
3,	4	420	435	449	449	446	445
4,	14	360	369	379	379	378	377
4,	20	370	369	370	370	370	370
9,	7	391	402	403	403	402	402
7,	31	308	303	291	291	293	294
10,	32	290+	312	309	309	310	310
14,	28	312	333	341	341	338	337
[1]10,	39	296	298	282	283	287	289
[1]15,	39	296	310	284	286	292	295
[1]16,	39	296	310	284	286	292	295
[1]17,	39	296	310	284	286	292	295
26,	56	279	271	213	215	224	231

[1]Multiaquifer well. Observed head is a composite of the heads in two subregional aquifers.

Downward hydraulic gradients are relatively steep near the major divide. Conversely, upward gradients increase with proximity to the regional drain. Lines of equal hydraulic head seem to be largely vertical within aquifers but are relatively curved in the vicinity of local points of net recharge and discharge and near confining units. Accordingly, the qualitative flow lines are largely horizontal within aquifers and relatively curvilinear near confining units and near streams. Flow lines toward nodes 6,55 and 6,56, which represent the regional drain, indicate that ground-water discharge to the Ocmulgee River is largely the result of direct flow from sediments equivalent to the Tallahatta-Gordon aquifer and indirect flow from the Clayton-Ellenton, Providence Sand-Peedee, and Eutaw-Midville aquifers.

Computed net rates of ground-water recharge and discharge are summarized in tables 3 and 4. Mean annual net recharge was about 6 in/yr. Corresponding maximum rates of net recharge and discharge were about 18 and 20 in/yr, respectively. Net discharge to the regional drain equaled about 7 percent of the total net recharge to the cross-section model. Computed net discharge occurred to the three tributary streams which intersect the cross-section path line at about miles 6.0, 15.5, and 17.5. These streams named, respectively, Mule Creek, Donelson Branch, and Redding Branch received ground-water flow at computed rates ranging from about 0.3 to 0.6 $(ft^3/s)/mi$. Significant rates of discharge also were shown to occur at topographic lows where actual streams were ephemeral or where wetlands were noted on topographic maps. Discharge to wetland areas is considered a loss to evapotranspiration.

Table 3.--Sensitivity of computed maximum ground-water recharge rates to changes in model anisotropy--cross-section models 1 and 2

[Trpy, anisotropy ratio]

	Maximum computed recharge rate, in inches per year				
	Trpy = 0.005	Trpy = 0.05	Trpy = 1.0	Trpy = 0.1	Trpy = 0.5
Cross-section model 1	17.8	54.8	239.1	80.2	166.9
Cross-section model 2		19.4	82.6	28.3	43.9

Net rates of ground-water discharge and recharge are highly variable along the water table with differences of two orders of magnitude occurring between respective maximum and minimum rates (table 4). A well-defined hinge line occurred at about mile 15.5 separating general areas of net ground-water recharge (which occurs at a total of 29 nodal cells) and discharge (which occurs at 27 nodal cells). Net discharge occurs for the most part at water-table nodes between the hinge line and the regional drain; whereas net recharge occurs most commonly at nodes between the major divide and the hinge line.

Table 4.--Computed ground-water net recharge and discharge rates using calibrated values of hydraulic conductivity and model anisotropy--cross-section model 1

Mean annual recharge and discharge (inches per year)	Maximum annual recharge (inches per year)	Minimun annual recharge (inches per year)
6.1	17.8	0.08

Maximum annual discharge (inches per year)	Minimum annual discharge (inches per year)	Mean annual discharge to regional drain (cubic feet per second per mile)
20.4	0.21	0.42

Ratio of discharge to regional drain to total recharge (percent)
6.5

Examination of cross-section model 1 results (pl. 6) indicates that the simulated regional subsystem can be qualitatively subdivided by flow regime. A well-defined regional flow regime appears in the basal part of the subsystem bounded by the Ripley-Black Creek confining unit and the base of the regional subsystem. Additionally, the water-table configuration seems to greatly influence the distribution of ground-water flow to a depth near the top of the uppermost confining unit. Flow in this zone between the water table and the top of the uppermost confining unit perhaps can best be described as both local and intermediate. Although distinct local flow systems cannot be exactly differentiated, several probable local flow systems are shown on plate 6 related to Mossy Creek, Donelson Branch, and near the wetland west of the hinge line.

Cross-section model 2

Cross-section model 2 (fig. 5) extends from the major divide of a regional subsystem near New Ellenton in Aiken County, S.C., to the Savannah River near Jackson in Aiken County, S.C. The cross-section line is about 16 miles long as measured on 7 1/2-minute topographic maps (pl. 1). Geohydrologic control along the line of the cross section was obtained from three boreholes that penetrate all or nearly all of the Coastal Plain sediments at cross-section miles 0.5, 6.5, and 13.5 (pl. 1; fig. 5).

The uppermost component subregional aquifer represents the combined Barnwell-Upper Floridan and Tallahatta-Gordon aquifers (Miller and Renken, 1988). The middle component aquifer is inclusive of the Clayton-Ellenton and Providence Sand-Peedee aquifers. The Eutaw-Midville subregional aquifer is the basal aquifer of the cross-section model. The upper and middle aquifers are separated by the Porters Creek-Ellenton subregional confining unit. The middle and basal aquifers are separated by the Ripley-Black Creek subregional confining unit. The base of cross-section model 2 is the top of consolidated Piedmont rocks (fig. 5).

The vertical distribution and thickness of component aquifers and confining units are shown in figure 5. Confining-unit sediments are rarely thicker than 50 ft. The thickness of aquifer sediments ranges from about 100 to 400 ft.

Lateral hydraulic conductivity of the aquifers in the calibrated model ranges from about 5 to 35 ft/d and was based on transmissivities computed at three sites near the cross section at mile 7.0 and at the terminal point of the path line at mile 16.0. Two of the site tests near mile 16.0 were comprehensive multiple-day aquifer tests utilizing a minimum of three observation wells. Aquifer-test data pertained exclusively to sediments of the Eutaw-Midville aquifer and included both time-drawdown and time-recovery information (Faye and McFadden, 1986). Hydraulic conductivities of other aquifer units were estimated from descriptions of sediment lithology. Nodally distributed values of hydraulic conductivity used in the calibrated model are shown in figure 6. Corresponding values of specified water-table head are listed in table 5. The subregional confining units seem to extend most of the length of the cross section (fig. 5).

Table 5.--Nodally distributed values of water table head--cross-section model 2

Specified head values, in feet					
Cross-section model two					
Row	Column	Head	Row	Column	Head
7	1	82	4	17	217
7	2	90	4	18	220
7	3	100	4	19	230
6	4	105	4	20	233
6	5	109	4	21	226
6	6	108	4	22	239
6	7	119	4	23	245
6	8	120	3	24	257
6	9	122	3	25	253
6	10	130	3	26	251
6	11	145	3	27	261
5	12	150	3	28	252
5	13	160	3	29	265
5	14	180	3	30	263
5	15	190	3	31	253
4	16	200	3	32	268

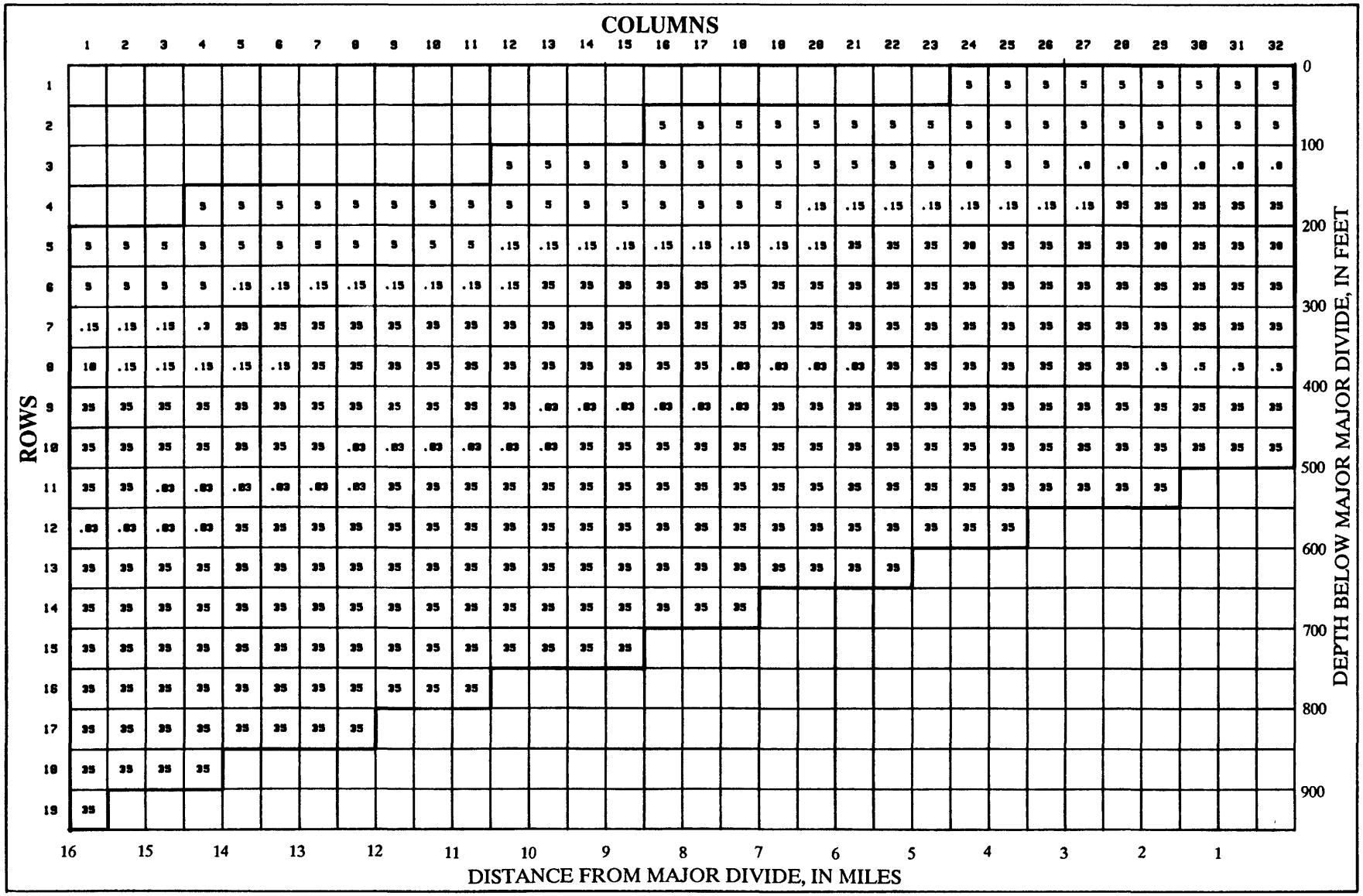

Figure 6.--Nodally distributed values of lateral hyraulic conductivity, in feet per day for cross section model 2.

Table 6.--Sensitivity of computed hydraulic head to changes in model anisotropy--cross-section model 2

[Trpy, model anisotropy]

Node row, column		Observed hydraulic head (feet)	Computed hydraulic head, in feet			
			Calibrated anisotropy (Trpy = 0.05)	Trpy = 1.0	Trpy = 0.1	Trpy = 0.5
4,	24	234	256	257	257	257
5,	18	213	220	220	220	220
6,	14	180	180	180	180	180
7,	4	115	105	105	105	105
8,	17	208	205	214	212	207
9,	19	223	221	228	227	223
10,	4	125	110	105	105	107
18,	5	161	144	108	111	129
4,	32	260	267	268	268	267
8,	31	258	259	255	256	259

Lateral hydraulic conductivity of confining units used in the calibrated cross-section model ranged from 0.03 to 0.15 ft/d. The calibrated model anisotropy is 0.05. Thus, leakance of model confining units ranges from about 10^{-5}/d to 10^{-4}/d.

The model-computed distribution of hydraulic potential and selected qualitatively derived flow lines are shown in figure 5. Observed hydraulic heads and corresponding computed heads are listed in table 6. Observed hydraulic heads are well distributed within the cross section and, except at nodal cells 4,24 and 18,5, heads computed by the calibrated cross-section model match observed heads within the 15-foot calibration limit. Computed rates of maximum net recharge and discharge are about 19 and 20 in/yr, respectively, at a model anisotropy of 0.05 (tables 3 and 7).

Table 7.--Computed ground-water net recharge and discharge rates using calibrated values of hydraulic conductivity and model anisotropy--cross-section model 2

Mean annual recharge and discharge (inches per year)	Maximum annual recharge (inches per year)	Minimum annual recharge (inches per year)
7.9	19.4	0.21
Maximum annual discharge (inches per year)	**Minimum annual discharge (inches per year)**	**Mean annual discharge to regional drain (cubic feet per second per mile)**
19.9	0.20	0.70
Ratio of discharge to regional drain to total recharge (percent)		
17.2		

Net rates of ground-water recharge and discharge are summarized in table 7. Computed mean annual recharge was about 8 in/yr. Net ground-water discharge to the regional drain (Savannah River) totaled about 17 percent of total subsystem recharge. This percentage is more than twice the corresponding percentage computed for cross-section model 1. Two factors may be partly responsible for this difference. The generally greater aquifer transmissivity in cross-section model 2 compared with cross-section model 1 along similar or greater potential

gradients may be reflected in higher rates of ground-water flow in the latter model. Additionally, a large number of tributary streams in cross-section model 1 intercept a relatively large percentage of total flow; whereas, no significant tributary streams occur along the line of cross-section model 2. Thus, a greater percentage of total flow would be expected to discharge to the regional drain. The lack of well-defined tributaries in cross-section model 2 is manifest in the lack of local flow systems shown in figure 5. Accordingly, flow lines shown in cross-section model 2 may largely represent intermediate and regional flow components.

A well-developed hinge line occurs in cross-section model 2 at about mile 7.0 near the edge of a sharp break in the water-table configuration. This break corresponds to a sharp change in topography at the eastern edge of an extensive flood plain that borders the Savannah River (fig. 5). Computed net ground-water recharge occurs at a total of 13 nodes along nearly the entire length of the water table between the hinge line and the major divide. Conversely, net ground-water discharge occurs almost exclusively along the water table between the hinge line and the regional drain. Computed net discharge is pronounced across the flood plain between miles 10.5 and 16.0 (fig. 5).

The simulated flow system at cross-section model 2 closely resembles that described for cross-section model 1. The water-table configuration seems to significantly influence the distribution of hydraulic head down to the top of the uppermost confining unit. Vertical hydraulic-head gradients are largely downward upstream of the hinge line and upward between the hinge line and the regional drain. Vertical changes in hydraulic head across confining units are most pronounced within that part of the subsystem underlying the flood plain and the regional drain.

Exaggerated potentiometric lines within aquifers are vertical except in the vicinity of the flood plain and the regional drain where there is a relatively high degree of curvature. Flow lines toward nodes 7,1 and 7,2, which represent the regional drain, indicate that discharge to the Savannah River occurs directly from sediments of the combined Barnwell-Upper Floridan and Tallahatta-Gordon aquifers and indirectly from the Eutaw-Midville aquifer.

Sensitivity Analyses

Errors in aquifer characteristics or boundary conditions assigned to the model affect the accuracy of model simulations. Inaccuracies in model boundaries are most likely to occur in the specification of the water-table configuration and in the imposition of zero-flow conditions at the major divide and the regional drain of the regional subsystem.

An alternative approach to modeling the water-table configuration requires the application of total recharge rates to the water-table nodes while the model computes the hydraulic head at the nodes. Actual local field-recharge rates in the study area are virtually unknown. Thus, the results of model simulations using applied recharge rates would be characterized by a significantly higher degree of uncertainty than those based on a specified definition of water-table potential.

Similarly, a test of the zero-flow condition imposed at the major divide and regional drain can be achieved by substituting specified-head conditions at each boundary node. Measurements of hydraulic-head at various depths under near predevelopment conditions at the boundary locations are not available.

Accordingly, simulations using estimated heads at the boundaries or estimates of field recharge rates at the water table would provide little, if any, insight into the validity of calibrated model results.

The sensitivity of model results with respect to changes in model anisotropy are summarized in tables 2, 3, and 6. Because the cross-section models are fully constrained at the boundaries, including a water table defined by specified heads, changes in computed hydraulic head with changes in model anisotropy are not particularly extreme (tables 2 and 6). On the other hand, computed rates of ground-water flow were highly sensitive to changes in model anisotropy. For example, computed rates of maximum net recharge to cross-section model 1 ranged from about 18 in/yr at a model anisotropy of 0.005 to about 240 in/yr at an anisotropy of 1.0 (table 3). Similar and corresponding changes occurred in rates of computed net discharge. Tests of model simulations with respect to changes in hydraulic conductivity were accomplished by uniformly varying the calibrated conductivity of cross-section model 1 by factors of 0.5, 2.0, and 10.0. The results of these tests with respect to the sensitivity of computed heads and maximum computed net recharge rates are shown in tables 8 and 9, respectively, and closely parallel those shown for model anisotropy.

In summary, computed net rates of ground-water recharge and discharge were sensitive to changes in both sediment hydraulic conductivity (table 9) and model anisotropy (table 3). Order-of-magnitude changes in either parameter resulted in corresponding order-of-magnitude changes in computed net flow rates. Conversely, corresponding changes in computed hydraulic head were minimal (tables 2, 6, and 8). Similar tests were conducted for cross-section model 2 and similar results were obtained.

Additional insight into the sensitivity of cross-section model results to contrasts in aquifer characteristics can be gained by varying the hydraulic conductivity of confining units while maintaining aquifer conductivities at original or near original values. Accordingly, a schematic model was developed wherein all aquifer nodal cells of cross-section model 1 were assigned a lateral hydraulic conductivity of 10 ft/d. Lateral conductivity at confining unit cells was also equal throughout the model but was varied per simulation between 0.01 and 10.0 ft/d. Model anisotropy was held constant at the calibrated value of 0.005. Computed mean annual flow for the schematic model varied somewhat over the range of confining unit conductivities from about 10 to 14 in/yr. Changes in flow were proportional to changes in confining unit conductivity but not directly. Mean annual flow rates simulated by the schematic model are somewhat high compared to the rate computed by the calibrated version of cross-section model 1 (table 4). This increase is probably due to the conductivity values used in the schematic model in the vicinity of the water table which at many nodal cells are a factor of four or more greater than corresponding values used in the calibrated model.

Changes in computed hydraulic head values in conjunction with changes in confining unit lateral conductivity ranged from greater than 100 ft in the Eutaw-Midville aquifer in the downstream part of the schematic model to

virtually zero in nodes near the water table (table 10). Divergence between heads computed by the schematic model and observed hydraulic heads increased with decreasing confining unit conductivity less than 0.1 ft/d and increasing conductivity greater than 1.0 ft/d. Divergence between observed and simulated heads was most pronounced in the downstream parts of the Eutaw-Midville aquifer.

Because model anisotropy was held constant and equal to 0.005 for each schematic model simulation, the effective anisotropy or the contrast in vertical hydraulic conductivity between the aquifers and confining units changed in direct proportion to changes in confining unit lateral conductivity. Accordingly, effective anisotropy equaled model anisotropy at a confining unit conductivity of 10 ft/d and was three orders of magnitude smaller at a confining unit conductivity of 0.01 ft/d.

Table 8.--Sensitivity of computed hydraulic head to changes in hydraulic conductivity--cross-section model 1

[TRNC, calibrated hydraulic conductivity]

Node row, column	Observed hydraulic head (feet)	Computed-hydraulic head, in feet			
		1.0 x TRNC	0.5 x TRNC	2.0 x TRNC	10.0 x TRNC
2, 4	423	438	438	438	438
3, 4	420	435	435	435	435
4, 14	360	369	369	369	369
4, 20	370	369	369	369	369
9, 7	391	402	402	402	402
7, 31	308	303	303	303	303
10, 32	290+	312	312	312	312
14, 28	312	333	333	333	333
10, [1]39	296	298	298	298	298
15, [1]39	296	310	310	310	310
16, [1]39	296	310	310	310	310
17, [1]39	296	310	310	310	310
26, 56	279	271	271	271	271

[1]Multiaquifer well. Observed head is a composite of heads in two subregional aquifers.

Table 9.--Sensitivity of computed maximum net ground-water recharge rates to changes in hydraulic conductivity--cross-section models 1 and 2

[TRNC, calibrated hydraulic conductivity]

	Maximum computed recharge rate, in inches per year			
	1.0 x TRNC	0.5 x TRNC	2.0 x TRNC	10.0 x TRNC
Cross-section model 1	17.8	8.8	35.5	177.3
Cross-section model 2	19.4	9.7	38.9	194.8

The results of the schematic model simulations indicate that changes in effective anisotropy affect computed hydraulic head to a significantly greater degree than they affect computed total flow rates. Part of this result is probably a consequence of cross-section model geometry, particularly the lack of confining units in the upstream part of the cross section where considerable recharge occurs to the model (pl. 6). Additionally, simulations of hydraulic head which best match the field observations for cross-section model 1 occurred using confining unit lateral conductivities between 0.1 and 1.0 ft/d. This conclusion is based largely on comparisons of observed and computed heads in the mid and downstream parts of the Eutaw-Midville aquifer at nodal cells 26,56 and 15-17,39. This range of conductivity values closely corresponds to the confining unit conductivities used in the calibrated version of cross-section model 1.

Comparison to Conceptual Model

Many of the elements of the literature-based conceptual model of ground-water flow were apparent in the results of the calibrated cross-section models. Cross-section model results also suggested several minor modifications to the conceptual model.

Flow regimes --

The cross-section model investigations suggest that the base of the local flow regime closely corresponds to the top of the uppermost subregional confining unit (pl. 6; fig. 5). Where such confinement does not occur, local flow regimes appear to extend to about one half the cross-section thickness.

Net recharge and discharge --

Net recharge and discharge were shown to occur largely in highland and lowland areas, respectively (pl. 6; fig. 5). Net recharge and discharge distributions were also highly variable along water-table configurations (tables 4 and 7).

Table 10.--Sensitivity of schematic model results to changes in lateral hydraulic conductivity of confining units

[Trpy = 0.005]

[CUHC = confining unit hydraulic conductivity]

Node row, column	Observed hydraulic head (feet)	Computed hydraulic head, in feet					
		CUHC = 0.01	CUHC = 0.05	CUHC = 0.1	CUHC = 0.5	CUHC = 1.0	CUHC = 10.0
2, 4	423	444	444	444	444	444	444
3, 4	420	440	440	440	440	440	440
4, 14	360	373	373	373	373	373	372
4, 20	370	371	370	371	371	371	370
9, 7	391	406	404	404	402	401	399
7, 31	308	299	299	299	300	300	302
10, 32	290	312	308	307	306	307	308
14, 28	312	368	343	336	331	332	334
[1]10, 39	296	301	299	298	291	289	286
[1]15, 39	296	360	328	315	297	293	289
[1]16, 39	296	360	328	316	297	293	289
[1]17, 39	296	360	328	316	297	294	289
26, 56	279	356	318	302	269	258	240

[1] Multiaquifer well. Observed head is a composite of the heads in two subregional aquifers.

Model anisotropy --

Increases in model anisotropy were shown to increase the quantities of net ground-water discharge and recharge (table 3). Corresponding changes in the relative distribution of net recharge and discharge along the water-table configuration were not apparent.

Stream and ground-water relations --

The conceptual descriptions regarding the distribution of ground-water flow to the regional drain and smaller streams were, to a large degree, duplicated by the cross-section model simulations. Net discharge to the regional drain appears to occur largely from ground-water flow that traverses all or most of the length of the regional subsystem and equals a relatively small percentage of total flow through the regional subsystem.

Fluid potential --

The water-table configuration of each calibrated cross-section model was deliberately designed to conform uniformly to topography and was held constant for each model. This boundary constrained and, to an unknown degree, biased the model results. However, given this bias, the model simulations largely support the conceptual descriptions of fluid potential. The influence of the water-table configuration on the distribution of fluid potential within the shallow part of the cross section was particularly apparent as were the large and directionally opposite hydraulic gradients associated with local topographic highs and lows. A general decrease in fluid potential near the major subsystem divide and an increase in the vicinity of the regional drain was characteristic of each calibrated model.

Application to Areal Studies

The variability of net ground-water recharge simulated along the water-table configuration by the calibrated cross-section models suggests that corresponding net recharge rates applied to areal models should be spatially variable. Additionally, cross-section flow model investigations suggest that net recharge to regional flow systems occurs at the major drainage divides and within the upstream parts of regional subsystems. Thus, areal simulations of regional or areally extensive ground-water flow that apply uniform or nearly uniform rates of net recharge to entire outcrop areas without regard to topographic configuration or the concepts of ground-water flow in a regional subsystem could misrepresent the hydrology of the model area.

Fluid-potential distributions within the local flow systems of the calibrated cross-section models are characterized by large but directionally opposite hydraulic gradients beneath local topographic highs and lows. Such distributions indicate that potentiometric data obtained from shallow wells in and near outcrop areas may not represent the average head in the aquifer, being below average near the stream valleys and above average near drainage divides. Potentiometric surface maps based on such data are commonly used in the calibration of areal flow models. Thus, for example, those areal model computations that closely match shallow well head data in stream valleys may be inaccurate and a simulation that computes higher than observed values may be more representative of average field conditions.

Mean Annual Baseflow

The Rorabaugh-Daniel stream hydrograph separation method was used to compute mean annual aquifer discharge to regional drains. A theoretical development and example application of this method are presented in Appendix I.

The Rorabaugh-Daniel method of hydrograph separation was applied to discharge records of paired continuous-record gages on the Chattahoochee River at Columbus, Ga. and Columbia, Ala.; on the Flint River at Culloden and Montezuma, Ga.; on the Ocmulgee River at Macon and Hawkinsville, Ga.; on the Oconee River at Milledgeville and Dublin, Ga.; on the Ogeechee River at Louisville and Scarboro, Ga.; and on the Savannah River at Augusta, Ga. (pl. 1). With the exception of the Ogeechee River gages, the upstream gage of each pair was located near the Inner Margin of Coastal Plain sediments. The location of the downstream station of each pair was near the edge of the outcrop area of clastic aquifer sediments. Thus, the area drained between the two gages contains most of the outcrop area of aquifers in the Georgia Subregion.

The streamflow discharge record for each of these stations was reviewed to determine the streamflow-recession index. Subsequently, rates of annual aquifer discharge to streams and to evapotranspiration were computed for major rise and recession periods at seven stations for selected years (table 11). At least 10 years of unregulated discharge record was available at each of the seven stations for this analysis. Long-term regulation of streamflow upstream of the Chattahoochee River gage at Columbus, Ga., precluded the computation of a recession index at this station. The recession index used for the Columbus station was computed using unregulated record at the upstream station at West Point, Ga. Comparison of coincident hydrographs indicates a strong correspondence between the major hydrograph features of both stations (fig. 7).

Net annual aquifer discharge to a regional drain gaging station was computed by summing the annual aquifer discharges for both the major rise and recession periods (described in Appendix I) and subtracting the discharge to evapotranspiration.

The relation between net annual aquifer discharge to the stream and aquifer discharge during the major rise period was evaluated by regression analysis using data listed in table 11. The resulting regression equation is

Net annual aquifer discharge to the stream = 1.04 (aquifer discharge for the major rise period) + 0.57.

The correlation coefficient and standard error of estimate of this equation are 0.98 and 0.36, respectively. This analysis indicates that a strong positive correlation probably exists between aquifer discharge to regional drains during the major rise period and net annual aquifer discharge.

Annual hydrographs representing "low," "average," and "high" years of stream discharge were subjectively selected for each of the nine regional drain gaging stations. Net aquifer discharge to the drain during the major rise period was computed for the three representative flow conditions at each station. Net annual aquifer discharge at each station for each representative

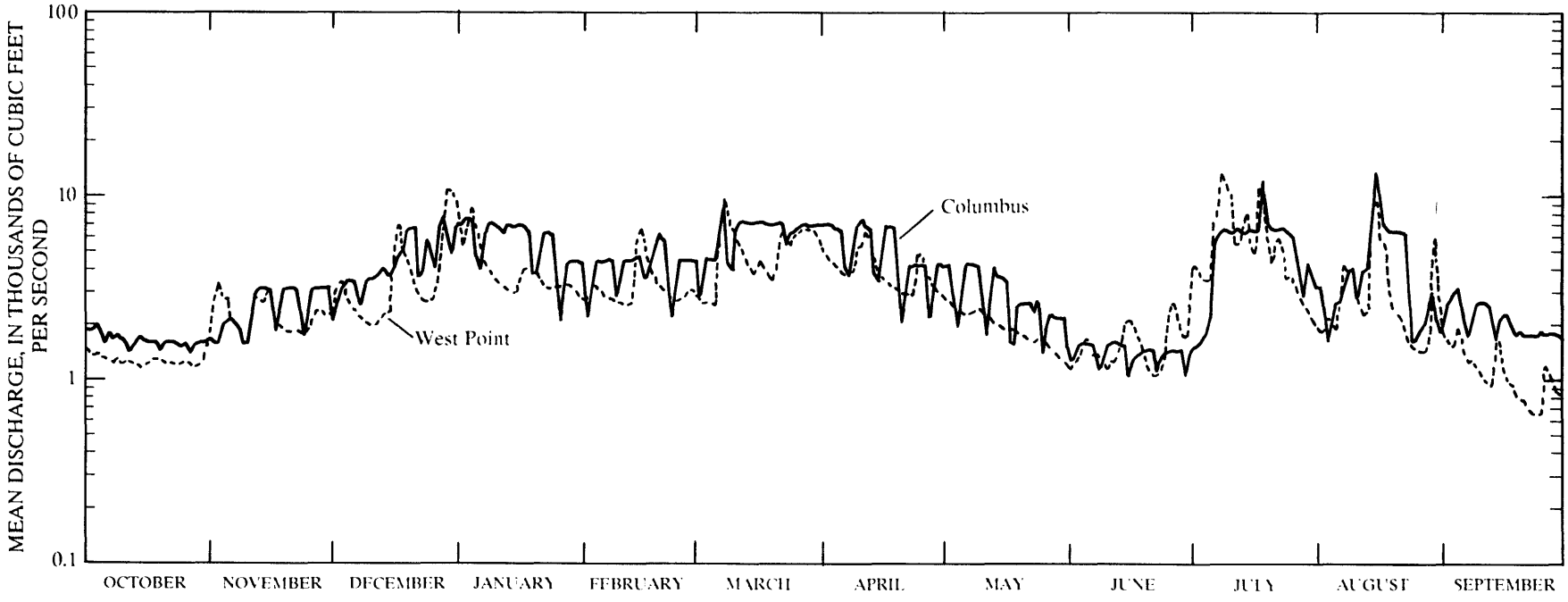

Figure 7.--Streamflow hydrographs of the Chattahoochee River at West Point and Columbus, Georgia, water year 1941.

Table 11.--Summary of annual aquifer discharge computed by hydrograph separation

Station name	Station number	Year	Drainage area (square miles)	Physiographic province	Aquifer discharge computed from annual hydrograph separation			
					Major rise period	Major recession period		
					Aquifer discharge (inches)	Aquifer discharge (inches)	Aquifer discharge to evapotranspiration (inches)	Net annual discharge to drain (inches)
Chattahoochee River at West Point, Ga.	02339500	1941	3,550	Piedmont	5.21	4.40	2.89	6.72
Chattahoochee River at West Point, Ga.	02339500	1952	3,500	Piedmont	9.60	2.28	1.60	10.28
Flint River near Culloden, Ga.	02347500	1941	1,850	Piedmont	4.02	1.00	.65	4.37
Ogeechee River at Scarboro, Ga.	02202000	1941	1,940	Coastal Plain	3.98	5.78	2.54	7.22
Ogeechee River near Louisville, Ga.	02200500	1941	800	Coastal Plain	4.65	1.95	.96	5.64
Ocmulgee River at Hawkinsville, Ga.	02215000	1931	3,800	Piedmont and Coastal Plain	3.92	1.69	.86	4.75
Ocmulgee River at Macon, Ga.	02213000	1905	2,240	Piedmont	3.40	1.52	1.05	3.87
Oconee River at Milledgeville, Ga.	02223000	1941	2,950	Piedmont	3.69	.84	.40	4.13

streamflow condition was then computed using the previously described regression equation. The mean annual aquifer discharge to the drain at each station was then computed as the average of the net annual aquifer discharges for the 3 years of "low," average," and "high" streamflow conditions.

Mean annual aquifer discharges at the selected regional drain gaging stations are listed in table 12. Other listed data include net streamflow gain between paired gaging stations normalized to a variety of units, the percent flow duration of mean annual aquifer discharge to the stream at each station, and computed annual evapotranspiration rate at several stations.

The lack of a well-defined recession for hydrographs at the Savannah River at Burtons Ferry Bridge, Ga., precluded the application of the Rorabaugh-Daniel method at this station. Accordingly, mean annual aquifer discharge was estimated by using reported net annual discharge gain between the gages at Augusta and Burtons Ferry Bridge (table 12) for the respective years at which hydrographs at the Augusta station were separated. Thus, the net gain listed in table 12 for the Savannah River between Augusta and Burtons Ferry Bridge is the maximum possible aquifer discharge for that reach.

Subregional Ground-Water Budget

In terms of both rates of ground-water flow and time of response, local ground-water flow regimes are probably most affected by climatic variability. Thus, during and particularly near the end of relatively long periods of little or no rainfall, the contribution of ground-water from local flow regimes to area streams is small or none and observed total streamflow at regional drain gages is probably largely the result of combined discharges from the intermediate and regional flow regimes. Although discharge from the intermediate flow regime is somewhat influenced by climate and is variable, it is relatively constant when compared to discharge from the local flow regime. Discharge from the regional flow regime is little affected by climatic variability and is nearly constant with time.

Comprehensive streamflow data were collected at regional drain gaging stations during droughts in water years 1941, 1954-55, and 1981. Table 13 summarizes these data on a daily or monthly basis near the end of one or more of the drought periods. At the time of these measurements, discharge from local flow regimes was considered zero and the net gains in discharge listed between the gaging stations represent total ground-water flow to the stream reach from the combined regional and intermediate flow regimes. Because of its relatively constant nature, this discharge (table 13) is further considered to be an approximation of total mean annual ground-water discharge from these combined flow regimes. Where several discharges are listed for the same reach, the smaller value is considered most representative of the mean annual ground-water discharge. Net discharge gain between gaging stations normalized over the respective intermediate drainage area is listed as a unit-area discharge. Average monthly streamflows were utilized for reaches of the Flint and Ocmulgee Rivers to account for short-term variations caused by upstream regulation. Other data related to regulated streams reflect relatively steady-state conditions at both the upstream and downstream gages for a substantial period prior to the reported measurement.

Table 13.--Summary of ground-water discharge to regional drains from combined intermediate and regional flow regimes based on drought streamflows

Regional drain		Intermediate drainage area (square miles)	Discharge (cubic feet per second)	Date	Net gain in discharge (cubic feet per second)	Unit area discharge (cubic feet per second per square mile)
Station name	Station number					
Chattahoochee River at Columbus, Ga.	02341500		[2]640	10-05-54		
		2,060			237	0.12
Chattahoochee River at Eufaula, Ala.	02342960		[2]877	10-05-54		
		840			243	.28
Chattahoochee River at Fort Gaines, Ga.	02343260		[1]1,120	10-05-54		
		470			250	.53
Chattahoochee River at Columbia, Ala.	02343500		[1]1,370	10-05-54		
Flint River near Culloden, Ga.	02347500		[3]315	09- -81		
		1,050			482	.46
Flint River at Montezuma, Ga.	02349500		[3]797	09- -81		
Flint River near Culloden, Ga.	02347500		[3]170	09- -54		
		1,050			532	.51
Flint River at Montezuma, Ga.	02349500		[3]702	09- -54		
		960			231	.24
Flint River at Oakfield, Ga.	02350500		[3]933	09- -54		

See footnotes at end of table.

Table 13.--Summary of ground-water discharge to regional drains from combined intermediate and regional flow systems based on drought streamflows--continued

Regional drain		Intermediate drainage area (square miles)	Discharge (cubic feet per second)	Date	Net gain in discharge (cubic feet per second)	Unit area discharge (cubic feet per second per square mile)
Station name	Station number					
Ocmulgee River at Macon, Ga.	02213000		[1]400	09-21-81		
		450			93	.21
Ocmulgee River near Warner Robins, Ga.	02213700		[1]493	09-21-81		
		370			87	.24
Ocmulgee River near Bonaire, Ga.	02214265		[2]580	09-21-81		
Ocmulgee River at Macon, Ga.	02213000		[3]165	10- -54		
		1,560			282	.18
Ocmulgee River at Hawkinsville, Ga.	02215000		[3]447	10- -54		
Oconee River at Milledgeville, Ga.	02223000		[3]438	10- -41		
		1,450			495	0.34
Oconee River at Dublin, Ga.	02223500		[3]933	10- -41		
Ogeechee River at Ga. Highway 16 near Shoals, Ga.	[4]105		[2].50	10-14-54		
		255			18.7	.073
Ogeechee River at Ga. Highway 24 near Louisville, Ga.	[4]106		[2]19.2	10-13-54		
		306			40.1	.13
Ogeechee River at Ga. Highway 4 near Louisville, Ga.	[4]113 02200500		[2]59.3	10-13-54		
		1,140			84	.073
Ogeechee River at Scarboro, Ga.	02202000		[1]143	10-13-54		

See footnotes at end of table.

Table 13.--Summary of ground-water discharge to regional drains from combined intermediate and regional flow systems based on drought streamflows--continued

Regional drain		Intermediate drainage area (square miles)	Discharge (cubic feet per second)	Date	Net gain in discharge (cubic feet per second)	Unit area discharge (cubic feet per second per square mile)
Station name	Station number					
Brier Creek at Ga. Highway 17 near Thomson, Ga.	[4]83 02197520		[2].01	10-14-54		
		116			21	.18
Brier Creek at Ga. Highway 4 near Blythe, Ga.	[4]86		[2]20.8	10-05-54		
		302			86	.28
Brier Creek at Ga. Highway 56 near Waynesboro, Ga.	[4]91 02197830		[2]107	10-04-54		
		173			0	0
Brier Creek at Millhaven, Ga.	02198000		[1]104	10-04-54		
Brier Creek at Ga. Highway 17 at Thomson, Ga.	[4]83 02197520		[1].83	09-30-81		
		418			83	.20
Brier Creek at Ga. Highway 56 near Waynesboro, Ga.	[4]91 02197830		[1]84	09-30-81		
		173			30	.17
Brier Creek at Millhaven, Ga.	02198000		[1]114	09-30-81		
Savannah River at Augusta, Ga.	02197000		[3]2,320	10- -41		
		1,140			660	0.59
Savannah River at Burtons Ferry Bridge near Millhaven, Ga.	02197500		[3]2,980	10- -41		

[1]Daily mean discharge.
[2]Discharge measurement.
[3]Monthly mean discharge.
[4]Thomson and Carter (1955).

Discharge to regional drains from local flow regimes should equal the difference between the total ground-water contribution to the drain and the combined discharge from the intermediate and regional flow regimes. Thus, for a common river reach, an estimate of mean annual ground-water discharge to regional drains from local flow regimes can be obtained by subtracting the combined intermediate and regional ground-water contribution (table 13) from the total mean annual ground-water discharge (table 12). These estimates are listed in table 14.

According to the conceptual model, discharge specifically from regional flow regimes occurs almost entirely to regional drains. Thus, an estimate of regional ground-water-flow rates can be computed by balancing mass over a short time interval in a downstream direction between regional drain gaging stations. A data base sufficiently comprehensive to permit such computations should necessarily include relatively concurrent daily measurements or estimates of discharge at the boundary gaging stations of the regional drain reach as well as estimates or measurements of tributary discharge to the same reach. In addition, flow conditions at measurement stations should be approximately steady state and representative of low flow or extreme low-flow conditions.

A base of streamflow data that reasonably conforms to these criteria is reported by Thomson and Carter (1955) and is partially summarized in table 15. Regional drain and tributary streamflow measurements are listed in table 15 for the Chattahoochee River, Flint River, Ogeechee River, and Brier Creek (fig. 1). Because of its length and drainage area, Brier Creek, a major tributary to the Savannah River in eastern Georgia, is considered a regional drain for purposes of computing the subregional hydrologic budget. All stations listed are located in the Coastal Plain except the most upstream stations on the Chattahoochee, Flint, and Ogeechee Rivers which drain only Piedmont rocks (table 15).

The total tributary discharge to a regional drain, reported in table 15, is calculated from a unit-area discharge extrapolated to the entire drainage of the stream. Each unit-area discharge is, in turn, based on a streamflow measurement that is generally inclusive of only part of the stream drainage. These measurements may not represent an average unit-area discharge for the entire tributary drainage, and accordingly, the estimate of total tributary contribution to the regional drain may be inaccurate. Nearly concurrent streamflow measurements at several stations on the same tributary are listed in table 15 for Hannahatchee and Pataula Creeks of the Chattahoochee River drainage, Rocky Comfort Creek of the Ogeechee River drainage, and Big Creek of the Brier Creek drainage. These measurements indicate a general downstream increase in unit-area discharge. Thus, estimates of total tributary discharge to the regional drain may be biased low where unit-area discharges are based on a relatively small percentage of the total tributary drainage area. Discharges from many of the large tributary streams listed in table 15 are based on streamflow measurements made near the mouths of the streams, and, accordingly, probably are representative of the entire tributary contributing area.

Estimates of streamflow listed in table 15 that are based on stage-discharge relations or unit-area discharges are considered accurate to within ±10 percent of the reported value. Estimates based on discharge measurements are considered accurate to within ±5 percent of the reported value.

Table 14.--Summary of ground-water discharge to regional drains from local flow regimes

Regional Drain		Intermediate drainage area	Estimated mean annual discharge gain from combined intermediate and regional flow systems based on drought streamflows	Mean annual unit area discharge from combined intermediate and regional flow systems	Total mean annual aquifer discharge gain based on hydrograph separation	Estimated mean annual gain from local flow systems	Mean annual unit area discharge from local flow systems
Station name	Station number	(square miles)	(cubic feet per second)	(cubic feet per second per square mile)	(cubic feet per second)	(cubic feet per second)	(cubic feet per second per square mile)
Chattahoochee River at Columbus, Ga.	02341500	3,370	[1]730	0.22	[2]2,840	2,110	.63
Chattahoochee River at Columbia, Ala.	02343500						
Flint River at Culloden, Ga.	02347500	1,050	[1]480	.46	[2]780	300	.28
Flint River at Montezuma, Ga.	02349500						
Ocmulgee River at Macon, Ga.	02213000	1,560	[1]280	.18	[2]890	610	.39
Ocmulgee River at Hawkinsville, Ga.	02215000						

See footnotes at end of table.

Table 14.--Summary of ground-water discharge to regional drains from local flow regimes--continued

Regional Drain: Station name	Regional Drain: Station number	Intermediate drainage area (square miles)	Estimated mean annual discharge gain from combined intermediate and regional flow systems based on drought streamflows (cubic feet per second)	Mean annual unit area discharge from combined intermediate and regional flow systems (cubic feet per second per square mile)	Total mean annual aquifer discharge gain based on hydrograph separation (cubic feet per second)	Estimated mean annual gain from local flow systems (cubic feet per second)	Mean annual unit area discharge from local flow systems (cubic feet per second per square mile)
Oconee River at Milledgeville, Ga.	02223000	1,450	[1]500	.34	[2]1,530	1,030	.71
Oconee River at Dublin, Ga.	02223500						
Ogeechee River at Louisville, Ga.	02200500	1,140	[1]84	.073	[2]620	540	.47
Ogeechee River at Scarboro, Ga.	02202000						
Savannah River at Augusta, Ga.	02197000	1,140	[1]660	.59	[2]1,220	560	.49
Savannah River at Burtons Ferry Bridge near Millhaven, Ga.	02197500						
Total		9,710	[1]2,730		[2]7,880	5,150	
Mean				.31			.50

[1]Table 13.
[2]Table 12.

Table 15.--Summary of ground-water discharge to regional drains based on streamflows measured during the drought of 1954

Regional Drain		Tributary Stream		Drainage area		Discharge	
Station name	Station number	Station name	Station number	(square miles)	Date	(cubic feet per second)	(cubic feet per second per square mile)
Chattahoochee River at Columbus, Ga.	02341500			4,670	10-05-54 10-12-54 10-14-54 10-26-54	[1]640, [2]640 [2]660 [2]660 [2]700	0.14
		Bull Creek at Ga. Highway 22 near Upatoi, Ga.	[3]740 [4]238	14.4	10-14-54	[1].90	.06
		Bull Creek at mouth at Columbus, Ga.	[4]241A	73.9		[5]5	--
		Upatoi Creek at Ft. Benning, Ga.	02342000 [3]777 [4]277	447	10-12-54	[1]121	.27
		Upatoi Creek at mouth of Ft. Benning, Ga.	[4]278	455	--	[6]123	--
		Uchee Creek near Ft. Mitchell, Ala.	02342500	325	10-05-54 10-12-54 10-14-54 10-26-54	[2]7.9 [2]7.2 [2]10 [2]9.6	.024
		Uchee Creek at Ft. Mitchell, Ala.	[7]18	334	--	[8]8	--
		Ihagee Creek at mouth near Holy Trinity, Ala.	[7]19	34.5	--	[8]1	--
		Hichitee Creek near Louvale, Ga.	[3]780 [4]284	39	10-26-54	[8]7.9	.20

See footnotes at end of table.

Table 15.--Summary of ground-water discharge to regional drains based on streamflows measured during the drought of 1954--Continued

Regional Drain		Tributary Stream		Drainage area		Discharge	
Station name	Station number	Station name	Station number	(square miles)	Date	(cubic feet per second)	(cubic feet per second per square mile)
		Hichitee Creek at mouth near Ft. Benning, Ga.	[6]284A	54.7	--	[9]11	--
		Hannahatchee Creek at Ga. Highway 1 near Louvale, Ga.	[3]781 [6]285	74	10-26-54	[1]1.24	.017
		Hannahatchee Creek near Julia, Ga.	783 [6]287	132	10-26-54	[1]17.7	.14
		Hannahatchee Creek at mouth near Omaha, Ga.	[6]287A	146	--	[10]20	--
		Hatchechubee Creek at mouth near Cottonton, Ala.	[7]22	151	--	[11]5	--
		Cowikee Creek at mouth near Eufaula, Ala.	[7]29	464	--	[11]16	--
		Chewalla Creek at mouth near Eufaula, Ala.	[7]30	28.6	--	[11]1	--
Chattahoochee River at Eufaula, Ala.	02342960			6,730		[1]877	[12]0.12
		Barbour Creek near Eufaula, Ala.	02343000	93.3	10-05-54 10-12-54 10-14-54 10-26-54	[2]3.2 [2]10 [2]12 [2]7.4	.034

See footnotes at end of table.

Table 15.--Summary of ground-water discharge to regional drains based on streamflows measured during the drought of 1954--Continued

Regional Drain		Tributary Stream		Drainage area		Discharge	
Station name	Station number	Station name	Station number	(square miles)	Date	(cubic feet per second)	(cubic feet per second per square mile)
		Barbour Creek at mouth near Eufaula, Ala.	[7]32	97.3	--	[1]3	--
		Cheneyhatchee Creek at mouth near Eufaula, Ala.	[7]33	56.6	--	[11]2	--
		Pataula Creek at Ga. Highway 1 near Lumpkin, Ga.	02343200 [3]786 [4]291	70	09-28-54	[1]12	.17
		Pataula Creek at Ga. Highway 50 near Georgetown, Ga.	02343225 [3]788 [4]294	295	09-27-54	90.7	.31
		Pataula Creek at mouth near Fort Gaines, Ga.	[4]296A	394	--	[13]120	--
		Cemochechobee Creek at Ga. Highway 39 near Fort Gaines, Ga.	[3]792 [4]299	103	10-21-54	[1]32.4	.31
		Cemochechobee Creek at mouth near Fort Gaines, Ga.	[4]299C	106	--	[14]33	--
Chattahoochee River at Fort Gaines, Ga.	02343260			7,570	10-05-54 10-11-54 10-14-54 10-21-54 10-26-54	[2]1,120 [2]1,060 [2]1,170 [2]1,070 [2]1,080	[15].29

See footnotes at end of table.

Table 15.--Summary of ground-water discharge to regional drains based on streamflows measured during the drought of 1954--Continued

Regional Drain		Tributary Stream		Drainage area		Discharge	
Station name	Station number	Station name	Station number	(square miles)	Date	(cubic feet per second)	(cubic feet per second per square mile)
		Kolomoki Creek at Ga. Highway 39	[3]794	[3]97	10-21-54	[1]56	.58
		Kolomoki Creek at mouth	[4]103	102	--	[1]59	--
		Abbie Creek near Haleburg, Ala.	02343300 [7]36	144	09-12-68	18	.13
		Abbie Creek at mouth	[7]37	196	--	[1]25	
Chattahoochee River at Columbia, Ala.	02343500			8,040	10-05-54 10-12-54 10-14-54 10-21-54	[2]1,370 [2]1,310 [2]1,340 [2]1,340	[1].53
Flint River near Culloden, Ga.	02347500			1,850	10-19-54 10-21-54 10-22-54	[2]97 [2]100 [2]100	0.054
		Culpepper Creek at Ga. Highway 7, near Roberta, Ga.	02348200 [3]853 [4]105	13	10-22-54	[1].18	.014
		Beaver Creek at mouth (east bank) near Reynolds, Ga.		78.9	--	[16]1	--
		Patsiliga Creek at Ga. Highway 128, near Reynolds, Ga.	02348300 [3]854 [4]108	139	10-22-54	[1]32.5	.23
		Patsiliga Creek at mouth near Reynolds, Ga.	[4]108A	142	--	[17]33	--

See footnotes at end of table.

Table 15.--Summary of ground-water discharge to regional drains based on streamflows measured during the drought of 1954--Continued

Regional Drain		Tributary Stream		Drainage area		Discharge	
Station name	Station number	Station name	Station number	(square miles)	Date	(cubic feet per second)	(cubic feet per second per square mile)
		Unnamed tributary near Nakomis, Ga.	[3]855 [4]109	12	10-22-54	[1].03	.003
		Unnamed tributary at mouth near Nakomis, Ga.		14.8	--	[18].04	--
		Beaver Creek at mouth (west bank), near Reynolds, Ga.		26.7	--	[17]6	--
		Horse Creek at Ga. Highway 128, near Marshallville, Ga.		29.6	10-21-54	[1]31.6	1.07
		Horse Creek at mouth near Marshallville, Ga.		36.6	--	[19]39	--
		Toteover Creek at mouth near Marshallville, Ga.		17.3	--	[16]19	--
		Whitewater Creek below Rambulette Creek near Butler, Ga.	02341900 [4]113	93.4	10-21-54	[2]132	1.41
		Whitewater Creek at mouth near Oglethorpe, Ga.	[4]117A	242	--	[20]342	--
		Buck Creek at U.S. Highway 11, near Ellaville, Ga.	02349350 [3]860 [4]120	146	10-19-54	[1]89.9	.62

See footnotes at end of table.

Table 15.--Summary of ground-water discharge to regional drains based on streamflows measured during the drought of 1954--Continued

Regional Drain		Tributary Stream		Drainage area		Discharge	
Station name	Station number	Station name	Station number	(square miles)	Date	(cubic feet per second)	(cubic feet per second per square mile)
		Buck Creek at mouth near Oglethorpe, Ga.	[4]121A	232	--	[21]143	--
Flint River at Montezuma, Ga.	02349500			2,900	10-19-54 10-21-54 10-22-54	[2]618 [2]618 [2]635	.49
Ogeechee River at Ga. Highway 16 at Jewell, Ga.	02200100 [3]105 [4]8			242	10-14-54	[1].50	.00
Ogeechee River at Ga. Highway 24 near Louisville, Ga.	02200130 [3]106 [4]12			495	10-13-54	[1]19.2	0.03
		Rocky Comfort Creek at Ga. Highway 80 near Gibson, Ga.	02200300 [3]110 [4]19	94	10-13-54	[1].30	.003
		Rocky Comfort Creek at Ga. Highway 24 at Louisville, Ga.	02200440 [3]112 [4]23	286	10-13-54	[1]46.7	.16
		Rocky Comfort Creek at mouth at Louisville, Ga.	[4]23A	288	--	47	--
Ogeechee River at Ga. Highway 4 near Louisville, Ga.	02200500 [3]113 [4]24			800	10-13-54	[1]59.3	[23].07

See footnotes at end of table.

Table 15.--Summary of ground-water discharge to regional drains based on streamflows measured during the drought of 1954--Continued

Regional Drain		Tributary Stream		Drainage area	Date	Discharge	
Station name	Station number	Station name	Station number	(square miles)		(cubic feet per second)	(cubic feet per second per square mile)
		Big Creek at Penns Bridge Road near Wrens, Ga.	[3]114 [4]25	8.1	10-06-54	[1]2.4	.30
		Big Creek at Middle Ground Road near Louisville, Ga.	[3]115 [4]26	56.9	10-06-54	[1]4.74	.08
		Big Creek at Ga. Highway 17 near Louisville, Ga.	02200900 [3]117 [4]28	95.8	10-13-54	[1]23.6	.25
		Big Creek at mouth near Louisville, Ga.	[4]28A	98.6	--	[24]25	--
		Williamson Swamp Creek at Ga. Highway 4, near Wadley, Ga.	[3]122 [4]37	232	10-15-5	[2]21.7	.094
		Williamson Swamp Creek at mouth near Wadley, Ga.		257	--	[25]24	--
		Rocky Creek at Ga. Highway 4 near Wadley, Ga.	[3]124 [4]39	11	10-15-54	[1]0	--
		Rocky Creek at mouth near Colemans Lake, Ga.		26	--	[26]0	--

See footnotes at end of table.

Table 15.--Summary of ground-water discharge to regional drains based on streamflows measured during the drought of 1954--Continued

Regional Drain		Tributary Stream		Drainage area		Discharge	
Station name	Station number	Station name	Station number	(square miles)	Date	(cubic feet per second)	(cubic feet per second per square mile)
		Clear Spring Creek at mouth near Colemans Lake, Ga.		15.2	--	[27]0	--
		Barkcamp Creek at Ga. Highway 17 near Hearndon, Ga.	[3]125 [4]41	32	09-10-54	[1]0	--
		Barkcamp Creek at mouth near Herndon, Ga.		36.1	--	[27]0	--
		Chew Mill Creek at Ga. Highway 17 near Herndon, Ga.	[3]126 [4]42	23	09-10-54	[1].23	0.01
		Chew Mill Creek at mouth near Herndon, Ga.		--	--	[28]0	--
		Dry Branch at Ga. Highway 17 near Herndon, Ga.	[3]127 [4]43	21	09-10-54	0	.0
		Buckhead Creek at mouth near Millen, Ga.		280	--	[29]10	--
		Sculls Creek at mouth near Scarboro, Ga.	[4]51A	82	--	[30]0	--
Ogeechee River at Scarboro, Ga.	02202000 [4]52			1,940	10-06-54 10-13-54 10-14-54 10-15-54	[2]143 [2]143 [2]143 [2]143	[31].0

See footnotes at end of table.

Table 15.--Summary of ground-water discharge to regional drains based on streamflows measured during the drought of 1954--Continued

Regional Drain		Tributary Stream		Drainage area		Discharge	
Station name	Station number	Station name	Station number	(square miles)	Date	(cubic feet per second)	(cubic feet per second per square mile)
Brier Creek at Ga. Highway 4 near Blythe, Ga.	[3]86 [4]158			171	10-05-54	[1]20.8	.12
		Boggy Gut Creek at mouth near Butler, Ga.		23.3	--	[32]7	--
		Sandy Run Creek near Blythe, Ga.	02197560 [3]87 [4]159	33.2	10-06-54	[1]11.1	.33
		Sandy Run Creek at mouth near Blythe, Ga.		35.5	--	[33]12	--
		Reedy Creek at mouth near Keysville, Ga.		56.5	--	[32]17	--
		Brushy Creek at Middle Ground Road near Matthews, Ga.	[3]90 [4]164	40.7	10-05-54	[1]10.5	.26
		Brushy Creek at mouth near Keysville, Ga.		64.1	--	[34]17	--
Brier Creek at Ga. Highway 56 near Waynesboro, Ga.	02197830 [3]91 [4]167			473	10-04-54	[1]107	[35]0.28

See footnotes at end of table.

[1]Discharge measurement.
[2]Mean daily discharge.
[3]Thomson and Carter (1955).
[4]Carter (1959).
[5]Estimate based on unit area discharge at Bull Creek at Ga. Highway 22.
[6]Estimate based on unit area discharge at Upatoi Creek at Ft. Benning, Ga.
[7]Stallings and Pierce (1957).
[8]Estimate based on unit area discharge at Uchee Creek near Ft. Mitchell, Ala.
[9]Estimate based on unit area discharge at Hichitee Creek near Louvale, Ga.
[10]Estimate based on unit area discharge at Hannahatchee Creek near Julia, Ga.
[11]Estimate based on unit area discharge at Barbour Creek near Eufaula, Ala.
[12]Unit area discharge computed using net discharge gain and intermediate drainage area between Chattahooche River stations at Columbus, Ga., and Eufaula, Ala.
[13]Estimate based on unit area discharge at Pataula Creek at Ga. Highway 50 near Georgetown, Ga.
[14]Estimate based on unit area discharge at Cemochechobee Creek at Ga. Highway 39 near Fort Gaines, Ga.
[15]Unit area discharge computed using net discharge gain and intermediate drainage area between Chattahooche River stations at Eufaula, Ala., and Fort Gaines, Ga.
[16]Estimate based on unit area discharge at Culpepper Creek at Ga. Highway 7 near Reynolds, Ga.
[17]Estimate based on unit area discharge at Patsigula Creek at Ga. Highway 128 near Reynolds, Ga.
[18]Estimate based on unit area discharge at unnamed tributary near Nakomis, Ga.
[19]Estimate based on unit area discharge at Horse Creek at Ga. Highway 128 near Marshallville, Ga.
[20]Estimate based on unit area discharge at Whitewater Creek below Rambulette Creek near Butler, Ga.
[21]Estimate based on unit area discharge at Buck Creek at U.S. Highway 19 near Ellaville, Ga.
[22]Unit area discharge computed using net discharge gain and intermediate drainage area between Flint River stations at Culloden, Ga., and Montezuma, Ga.
[23]Unit area discharge computed using net discharge gain and intermediate drainage area between Ogeechee Riv stations at Jewell, Ga., and at Ga. Highway 4 near Louisville, Ga.
[24]Estimate based on unit area discharge at Big Creek at Ga. Highway 17 near Louisville, Ga.
[25]Estimate based on unit area discharge at Williamson Swamp Creek at Ga. Highway 4 near Wadley, Ga.
[26]Estimate based on unit area discharge at Rocky Creek at Ga. Highway 4 near Wadley, Ga.
[27]Estimate based on unit area discharge at Bark Camp Creek at Ga. Highway 17 near Herndon, Ga.
[28]Estimate based on unit area discharge at Chew Mill Creek at Ga. Highway 17 near Herndon, Ga.
[29]Estimate based on measured flows tributary to Buckhead Creek reported in Thomson and Carter (1955, p. 53)
[30]Estimate based on measured flows tributary to Sculls Creek reported in Thomson and Carter (1955, p. 53).
[31]Unit area discharge computed using net discharge gain and intermediate drainage area between Ogeechee Riv stations at Ga. Highway 4 near Louisville, Ga., and at Scarboro, Ga.
[32]Estimate based on unit area discharge of 0.30 $(ft^3/s)/mi^2$.
[33]Estimate based on unit area discharge at Sandy Run Creek near Blythe, Ga.
[34]Estimate based on unit area discharge at Brushy Creek at Middle Ground Road near Matthews, Ga.
[35]Unit area discharge computed using net discharge gain and intermediate drainage area between Brier Creek stations at Ga. Highway 4 near Blythe, Ga., and Ga. Highway 56, near Waynesboro, Ga.

general condition of steady-state, the difference between total tributary discharge to a regional drain reach and the net gain in discharge determined by gaged streamflows at the reach boundaries over a short time-span should equate to ground-water discharge from the regional flow regime. Using data listed in table 15, such differences were determined to be small and generally within the error criteria of discharge measurements and estimates. Consequently, regional ground-water-flow rates are considered small relative to total low-flow rates and were determined by using a residual error analysis (table 16). Applying the error criteria noted previously, extremes of net gain and tributary contribution were computed. A range of regional aquifer discharge was then computed along with corresponding ranges of unit-area discharge (table 16).

Because there was no physical basis for determining which intermediate unit-area discharge best represents regional ground-water flow, the midvalue of the range of unit-area discharge was chosen as the value most likely to occur or most representative of regional ground-water flow for a particular reach of a regional drain. The high rate of regional ground-water discharge to the reach of the Chattahoochee River between Fort Gaines, Ga., and Columbia, Ala., probably is the result of ground-water flow to the reach from beyond the respective surface drainage boundaries. The unit-area discharge of this reach is considered unreasonably high and was not used in subsequent analyses.

The mean unit-area discharge from the regional ground-water flow regime is about 0.08 $(ft^3/s)/mi^2$ and is the mean of the sum of midvalues from each reach (table 16). The regional ground-water flow component contributed to regional drains can then be estimated as the product of mean unit-area discharge from the regional flow regime and the total intermediate watershed area of 9,710 mi^2 drained between the paired gaging stations listed in table 12. A rate of 780 cubic feet per second (ft^3/s) was calculated and is considered representative of the entire study area. Note that a regional flow rate of 780 ft^3/s equals about 10 percent of the total mean annual ground-water discharge to regional drains of 7,880 ft^3/s contributed for the same total intermediate watershed area (table 12).

A rate of regional ground-water flow which comprises about 10 percent of total ground-water flow within the study area compares favorably with the results of the cross-section model investigations. Discharge to the regional drains computed by the calibrated cross-section models equaled about 7 and 17 percent of total computed discharge. In addition, the discharge to the Ocmulgee River computed by cross-section model 1, which intersects the Ocmulgee River between the gages at Macon and Hawkinsville is about 6.3 $(ft^3/s)/mi$ (table 4). This rate compares well to the rate of 7.1 $(ft^3/s)/mi$ determined from ydrograph separation analyses and computed as one half the net gain listed in able 12 for the Ocmulgee River. Comparisons between cross-section model 2 and stimates of mean annual aquifer discharge to the Savannah River are not as irect. If all discharge to the flood plain computed by cross-section model 2 s considered ultimately to discharge to the Savannah River, then simulated round-water discharge to the regional drain equals about 2.2 $(ft^3/s)/mi$. is rate is low compared to the rate of 8.8 $(ft^3/s)/mi$ computed as one half e net gain for the Savannah River between Augusta and Burtons Ferry Bridge able 12). However, this rate of gain applies to total runoff, not just ifer discharge. Thus, a gain of about 2.0 $(ft^3/s)/mi$ may be appropriate regional ground-water flow to this part of the Savannah River. Such parisons indicate that the cross-section model results and elements of the ional hydrologic budget are mutually corroborative.

Table 16.--Summary of residual error computation of ground-water discharge from the regional flow regime

Regional Drain Station name	Station number	Intermediate drainage area (square miles)	Date	Range of discharge (cubic feet per second)	Range of net gain (cubic feet per second)	Range of tributary contribution (cubic feet per second)	Range of regional regime discharge (cubic feet per second)	Range of regional flow unit area discharge (cubic feet per second per square mile)	Unit area discharge range midvalue (cubic feet per second per square mile)
Chattahoochee River at Columbus, Ga.	02341500	2,060	10-05-54	610-670	120-360	[1]170-210	0-190	0.0-0.09	0.04
Chattahoochee River at Eufaula, Ga.	02342960	840	10-05-54	790-970	40-440	[1]140-180	0-300	0.0-0.36	.18
Chattahoochee River at Fort Gaines, Ga.	02343260	470	10-05-54 10-21-54	1,010-1,230 960-1,180	30-480	[1]76- 92	[2]0-400	0.0-0.85	.42
Chattahoochee River at Columbia, Ala.	02343500		10-21-54	1,210-1,470					
Flint River at Culloden, Ga.	02347500	1,050	10-21-54	90-110	450-590	[1]520-640	0- 70	0.0-0.07	.03
Flint River at Montezuma, Ga.	02349500		10-21-54	560-680					

See footnotes at end of table.

Table 16.--Summary of residual error computation of ground-water discharge from the regional flow regime--continued

Regional Drain Station name	Station number	Intermediate drainage area (square miles)	Date	Range of discharge (cubic feet per second)	Range of net gain (cubic feet per second)	Range of tributary contribution (cubic feet per second)	Range of regional regime discharge (cubic feet per second)	Range of regional flow unit area discharge (cubic feet per second per square mile)	Unit area discharge range midvalue (cubic feet per second per square mile)
Ogeechee River at Louisville, Ga.	0200500		10-13-54	56- 62					
		1,140			70-100	[1]53- 65	5- 50	0.0-0.04	.02
Ogeechee River at Scarboro, Ga.	02202000		10-13-54	130-160				0.0-0.07	.03
Brier Creek at Ga. Highway 4 near Blythe, Ga.	[2]158		10-05-54	20- 22				0.0-0.04	.02
		302			80- 90	[1]32- 40	40- 60	0.13-0.20	.16
Brier Creek near Waynesboro, Ga.	02197830		10-04-54	100-110					
		173			0- 14	No tributary contribution	0- 14	0.00-0.08	.04
Brier Creek at Millhaven, Ga.	02198000		10-04-54	94-114					
							MEAN		[4].08

[1]Table 15.

[2]Probably includes significant contribution from intermediate and regional flow systems which extend beyond the drain boundaries of the Chattahoochee River.

The elements of a subregional ground-water budget are listed in table 17. Total ground-water discharge to regional drains occurs at a mean annual rate of about 7,880 ft^3/s (0.81 $(ft^3/s)/mi^2$). Local and regional components of this discharge occur at the mean annual rates of 5,150 ft^3/s (0.53 $(ft^3/s)/mi^2$) and 780 ft^3/s (0.08 $(ft^3/s)/mi^2$), respectively. Mean annual discharge from intermediate flow regimes is, thus, estimated to occur at the rate of about 1,950 ft^3/s (0.20 $(ft^3/s)/mi^2$). Evapotranspiration losses from the ground-water system are estimated at about 660 ft^3/s (0.07 $(ft^3/s)/mi^2$) based on the mean of values of unit area discharge listed in table 11 applied to a total intermediate drainage area of 9,710 mi^2. The sum of these budget components is 8,540 ft^3/s which represents the recharge occurring to Coastal Plain sediments within the intermediate drainage areas of the paired gaging stations listed in table 12.

The remaining two flow components that have not been estimated are the quantity of ground-water flow that escapes discharge to any drain and proceeds downgradient into the southern half of the Coastal Plain and the subsurface inflow to the study area from Piedmont rocks across the Inner Margin of Coastal Plain sediments. Callahan (1964, p. 13) estimates that a likely discharge of about 0.75 ft^3/s per mile moves downgradient across a 400-mile width which spans the approximate downgradient limit of the study area. This discharge equals approximately 310 ft^3/s and is considered a reasonable value for downgradient discharge for this study. Inflow from the Piedmont rocks was estimated using a variant of Darcy's Law

$$Q = TIW$$

where

Q = ground-water discharge (L^3T^{-1});
T = aquifer transmissivity (L^2T^{-1});
W = width of the line of flow (L); and
I = flow gradient (LL^{-1}).

The flow gradient was estimated to be about 8.3 feet per mile based on published low-flow, water-surface profiles of several regional drains at the Inner Coastal Plain Margin (U.S. Corps of Engineers, 1945a, b; 1949a, b, c, d; 1959). Aquifer transmissivity was estimated to be 400 ft^2/d, based on published data by Stewart (1964) and Stewart and others (1964). The length of the Inner Coastal Plain Margin across the study area equals about 400 miles, which was considered the width of the line of flow. Accordingly, a discharge of about 20 ft^3/s was computed as a lateral flow contribution from Piedmont rocks to the study area. This rate is small compared to other elements of the hydrologic budget and is subsequently ignored for this study.

Thus, total ground-water recharge is estimated to occur at the mean annual rate of about 8,850 ft^3/s (0.91 $(ft^3/s)/mi^2$). Total recharge to the regional flow regime equals about 1,080 ft^3/s, based on the sum of the downgradient and regional flow component discharges (table 17).

Table 17.--Elements of the subregional ground-water budget

Mean annual ground-water discharge, in cubic feet per second					
Total recharge	Local flow regime	Intermediate flow regime	Regional flow regime	Evapotranspiration	Down-gradient discharge
8,850	5,150	1,950	780	660	310

Application to Areal Studies

The methods described in this section regarding the separation of stream-discharge hydrographs and the application of the conceptual model to seepage run data to determine elements of a ground-water budget generally can be applied at a variety of scales within the southeastern Coastal Plain and probably elsewhere. Investigators of areally extensive ground-water flow may take note of the limits placed on ground-water discharge to regional drains (table 12). For example, a calibrated areal model which simulates the regional component of ground-water flow should compute discharge to the Chattahoochee River between Columbus, Ga., and Columbia, Ala., at a rate substantially less than the 730 ft^3/s listed in table 14. Similarly, model computed net discharge from the regional flow regime to several regional drains should occur at an average unit-area rate not substantially different from 0.08 $(ft^3/s)/mi^2$).

In addition, the unit-area values computed for elements of the subregional ground-water budget (table 17) and components of aquifer discharge to regional drains (tables, 13, 14, and 16) probably can be considered representative of much of the clastic sediment outcrop area of the southeastern Coastal Plain when applied at an areally extensive or regional scale.

REGIONAL TRANSMISSIVITY DISTRIBUTION

Aquifer Diffusivity

Aquifer diffusivity is generally described as the ratio of transmissivity to storativity at a site. A more regional and less-constrained relation that describes diffusivity in terms of aquifer flow rate and potential at a stream gaging station was developed by Rorabaugh (1960). The general form of this relation is

$$T/S = \frac{0.933a^2 \log h_1/h_2}{t_2 - t_1} , \qquad (2)$$

where T is aquifer transmissivity, S is aquifer storativity, $\underline{a}$ is considered to approximate the average flow length of ground water to all perennial streams draining to the gage, and h_1 and h_2 are hydraulic potential in the aquifer at times t_1 and t_2. Diffusivity computed by equation (2) represents an integration or composite of component aquifer properties from the entire watershed contributing to the gaging station. For this study, diffusivity was determined at regional drain gaging stations and is termed a regional diffusivity. Related values of transmissivity and storativity are similarly described. Equation (2) is valid following a critical time period after which the streamflow (baseflow) recession is a straight line when plotted on semilogarithmic paper. Regional diffusivity is thus proportionally related to the slope of the linear streamflow recession by the factor $0.933\underline{a}^2$. If the difference t_2-t_1 equals the time in days required for stream stage (aquifer potential) to change 1 log cycle (table 12), then log h_1/h_2 in equation (2) equals 1.

Computation of aquifer diffusivity using equation (2) requires the determination of average flow length $\underline{a}$. Previous investigators (Trainer and Watkins, 1975; Daniel, 1976; and Stricker, 1983) have used the relation

$$\underline{a} = A/2L \qquad (3)$$

to estimate $\underline{a}$, where A is watershed drainage area and L equals total perennial stream length within the watershed. This relation is essentially average overland flow length in the watershed and is directly computed from drainage density (Leopold and others, 1964). Dingman (1978) argues that baseflow is not fundamentally related to drainage density but rather depends only on infiltration capacity and subsequent evapotranspiration. He further argues that the results of investigations purporting to demonstrate a strong correlation between baseflow and drainage density (Carlston, 1963) are fortuitous.

Investigations described herein, particularly the results of the cross-section flow models, tend to strongly support a lack of correspondence between drainage density and average ground-water flow length for those watersheds where intermediate and regional flow regimes substantially contribute to baseflow. Conversely, where baseflow is entirely or nearly entirely the result of discharge from a relatively shallow, local flow regime, average ground-water flow length may be well represented by drainage density and approximated using equation (3). Such conditions may be satisfied in the Georgia Subregion in small watersheds, perhaps those with drainage areas smaller than 10 mi^2.

Ground-water flow within the Piedmont occurs largely at shallow depth within the lower part of the regolith and is probably greatly influenced by local topography. Accordingly, overland flow length computed using equation (3) may also approximate average ground-water flow length in much of the Piedmont.

Drainage density for two large Piedmont watersheds within the upper Chattahoochee River basin was computed by Faye and others (1980) and averaged 2.22 mi^{-1}. This density transforms to an average overland flow length of about 1,200 ft. By comparison, Trainer and Watkins (1975) used a value of 1,250 ft as an estimate of $\underline{a}$ to compute aquifer diffusivity in Piedmont watersheds of the upper Potomac River basin. An average overland flow length of 1,200 ft was used in this study as an approximate value for $\underline{a}$ in Piedmont watersheds.

The computation of $\bar{a}$ at Coastal Plain regional drains (table 12) is necessarily subjective. Baseflow to regional Coastal Plain drains is comprised of significant contributions from the regional and intermediate flow regimes which are characterized by average or effective flowpaths of several to many miles in length. An established methodology to compute or estimate $\bar{a}$ under such circumstances presently does not exist. However, a range for $\bar{a}$ can be estimated by investigating the component parts of equation (2). Values of Coastal Plain aquifer transmissivity and storativity are generally known in the study area (Faye and McFadden, 1986) and range in magnitude from about 10^3 to 10^4 ft^2/d and 10^{-3} to 10^{-4}, respectively. In addition, values of Δt at regional drains have been shown to range from 10^1 to 10^2 days (table 12). Consequently, diffusivity of Coastal Plain aquifers which drain to major rivers appears to range between 10^6 and 10^8 ft^2/d. The quantity $0.933a^2$ then ranges between 10^7 and 10^{10} ft^2 and $\bar{a}$ is between 10,000 and 100,000 ft for ground-water flow to regional drain gaging stations.

Some insight into a truly representative value of $\bar{a}$ can perhaps be gained by measuring flow lengths on cross-section models 1 and 2 (pl. 6; fig. 5) and weighting these lengths using the local, intermediate, and regional flow regime discharges listed in table 17. To measure flow lengths, distances from recharge nodes along the water-table configuration to the locations of perennial streams were measured to the nearest half nodal length (1,320 ft). Local flow lengths were measured from the recharge node to the nearest perennial stream. Intermediate flow lengths were similarly measured but included one local flow system. Regional flow lengths were measured from recharge nodes along the major subsystem divide to the mid point of the regional drain. Measurements of local flow lengths were most numerous, totaling 38 for cross-section model 1 and 21 for cross-section model 2. Measurements of regional flow lengths were least numerous, totaling 7 and 14 for cross-section models 1 and 2, respectively. A summary of flow length measurements is presented below.

	Average flow length, in feet		
	Local regime	Intermediate regime	Regional regime
Cross section model 1	6,100	17,900	134,100
Cross section model 2	4,650	16,900	68,200

By weighting these lengths against the independently determined flow regime discharges listed in table 17, an average $\bar{a}$ of 26,100 ft was computed for cross-section model 1 and a corresponding length of 16,100 ft was computed for cross-section model 2. The regional flow regime discharge used in the weighting computation was 1,100 ft^3/s and equals the approximate sum of regional regime flow and downgradient discharge. Accordingly, an average length of ground-water flow of 21,000 ft was considered representative of regional drain watersheds within the study area.

Note that lines for cross-section models 1 and 2 cross numerous ephemeral streams. Had local flow lengths to these streams been considered, the average local flow length listed previously would have been considerably shorter. Conversely, intermediate flow frequently includes more than one local flow system. Had this condition been considered, the average intermediate flow lengths listed above would be considerably longer.

Values of a, streamflow-recession index, and computed aquifer diffusivity are listed in table 18 by regional drain gaging station. At stations which drain largely Piedmont watersheds the computed diffusivity is considered to be an effective average for the permeable volume of Piedmont rocks that ultimately deliver water to the regional drain. In addition, at the regional scale considered in this report, flow through the secondarily permeable Piedmont rocks is assumed to be substantially equivalent to flow through a porous media. At stations which drain both Piedmont and Coastal Plain watersheds, the computed diffusivity is considered to be largely representative of Coastal Plain aquifers.

Values of effective regional transmissivity within a watershed can be computed from diffusivity by using representative values of storativity. Within the study area, aquifer-test data that used one or more observation wells were available at a number of sites (Faye and McFadden, 1986). Tests at 10 sites were considered of sufficient quality to provide reasonable values of aquifer storativity which ranged from 1.5×10^{-4} to 3.1×10^{-3} and averaged 4.5×10^{-4}. Consequently, an average value of 5.0×10^{-4} was considered representative of Coastal Plain aquifer storativity within the study area.

Previous studies within the upper Potomac River basin by Trainer and Watkins (1975) indicate that gravity drainage probably characterizes ground-water flow in most Piedmont rocks and that 0.01 is a representative storativity value. A storativity of 0.01 is also considered characteristic of Piedmont rocks for this study.

Using the appropriate storativity and diffusivity values, average regional transmissivities of the Coastal Plain and Piedmont rocks were computed at regional drain gaging stations and are listed in table 18. Transmissivity of the Piedmont rocks ranges from about 100 to 200 ft^2/d and averages about 140 ft^2/d. Transmissivity was least in the Chattahoochee River watershed and greatest in the Oconee River watershed. These values are similar to the average transmissivity of Piedmont rocks computed by Trainer and Watkins (1975) using similar methodologies.

Average regional transmissivities of Coastal Plain sediments ranged from about 900 to 2,600 ft^2/d and averaged about 1,800 ft^2/d. These computed values are generally lower than observed aquifer transmissivity values for the study area (Faye and McFadden, 1986), the ranges of which are listed by watershed in table 18. The low values of transmissivity computed from diffusivity compared to those computed from aquifer-test data may be indicative of a selective bias on the part of aquifer-test values or unrealistically small values of storativity and/or ground-water flow length used in the diffusivity method computations. A poor comparison due to a bias of aquifer-test results is likely because aquifer-test data are limited in number and relate generally to large-capacity wells which obtain water from local, exceptionally permeable sections of aquifers. Bias caused by unrealistic flow length and storativity values is also possible. For example, a one mile increase in average

Table 18.--Summary of aquifer diffusivity analyses

Station name	Station number	Drainage area (square miles)	Streamflow-recession index Δt days	"a" (feet)	Diffusivity (square feet per day)	Average watershed transmissivity (square feet per day)	Range of observed local transmissivity (square feet per day)
Chattahoochee River at Columbus, Ga.	02341500	4,670	122	1,200	1.10×10^4	[1]110	NA
Chattahoochee River at Columbia, Ala.	02343801	8,040	222	21,000	1.85×10^6	[2]930	500- 6,900
Flint River near Culloden, Ga.	02347500	1,850	85	1,200	1.58×10^4	[1]160	NA
Flint River at Montezuma, Ga.	02349500	2,900	113	21,000	3.64×10^6	[2]1,820	500- 7,600
Ocmulgee River at Macon, Ga.	02213000	2,240	117	1,200	1.15×10^4	[1]115	NA
Ocmulgee River at Hawkinsville, Ga.	02215000	3,800	150	21,000	2.74×10^6	[2]1,370	4,000-37,000
Oconee River at Milledgeville, Ga.	02223000	2,950	62	1,200	2.17×10^4	[1]217	NA
Oconee River at Dublin, Ga.	02223500	4,400	105	21,000	3.92×10^6	[2]1,960	2,700-34,000
Ogeechee River near Louisville, Ga.	02200500	800	94	21,000	4.38×10^6	[1]2,190	--
Ogeechee River at Scarboro, Ga.	02202000	1,940	80	21,000	5.14×10^6	[2]2,570	[3]7,100
Savannah River at Augusta, Ga.	02197000	7,508	117	1,200	1.15×10^4	[1]115	NA

[1]Representative storage coefficient = 0.01.
[2]Representative storage coefficient = 5.0×10^{-4}.
[3]Single test.

ground-water flow length or a 50 percent increase in storativity will increase computed regional transmissivity by 50 percent. Given this sensitivity, the regional transmissivity values listed in table 18 should be considered useful in determining spatial trends and relative spatial differences in transmissivity within the study area but may not be absolute evaluations of effective regional transmissivity.

Application to Areal Studies

The distribution of regional transmissivity by watershed indicates a trend of increasing transmissivity west to east across the study area (table 18). This trend and the relative differences in regional transmissivity from watershed to watershed should be generally duplicated in subregional areal model investigations. In addition, the low value of regional transmissivity computed for Piedmont rocks compared to corresponding values for Coastal Plain sediments suggests that cross-section and areal models of Coastal Plain aquifers may reasonably consider the Inner Coastal Plain Margin and the base of Coastal Plain sediments as boundaries of little or no ground-water flow.

SUMMARY AND CONCLUSIONS

Investigations of ground-water flow within outcrop areas of clastic sediments of the Georgia Subregion RASA qualitatively and quantitatively described local, intermediate, and regional flow regimes and stream-aquifer relations. A literature-based conceptual model of ground-water flow for areally extensive aquifers was developed and tested using cross-section model analyses and site data. Major elements of the conceptual model indicated that:

(1) Water-table configurations are a subdued replica of surface topography and significantly influence the spatial distribution of net ground-water recharge and discharge and fluid potential;

(2) net ground-water recharge and discharge are spatially variable, perhaps to a great degree;

(3) fluid potential in the vicinity of major divides decreases with depth. Potential increases with depth in the vicinity of major drains; and

(4) discharge from the regional flow regime occurs largely to the regional drain and originates at or near the major subsystem divide.

Streamflow hydrographs were successfully separated into surface runoff and baseflow components at selected gaging stations on regional drains using the Rorabaugh-Daniel method. Total baseflow to regional drains was determined to occur at a mean annual rate of 7,880 ft^3/s. Seepage run and drought flow data in conjunction with results of the conceptual model analyses were used to calculate the local, intermediate, and regional components of total baseflow. These components included 5,150 ft^3/s of local flow; 1,950 ft^3/s of intermediate flow; and 780 ft^3/s of regional flow. Other elements of the hydrologic budget included a 660 ft^3/s loss to evapotranspiration and 310 ft^3/s of downgradient flow to the southern part of the Coastal Plain. Evapotranspiration was computed as part of the hydrograph separation analysis.

Computation of aquifer diffusivity at regional drain gaging stations indicates that transmissivity increases generally west to east across the study area.

REFERENCES

Bates, R. L. and Jackson, J. A., editors, 1980, Glossary of geology: American Geological Institute, 751 p.

Bechtel Corporation, 1973, Preliminary safety analysis report, vols. II and III--Alvin W. Vogtle Nuclear Plant: Atlanta, Georgia, Unpublished report prepared for Georgia Power Company.

Bennett, G. D., 1979, Regional groundwater systems analysis: Water Spectrum-U.S. Army Corps of Engineers, p. 36-42.

Bingham, R. H., 1982, Low-flow characteristics of Alabama streams: U.S. Geological Survey Water-Supply Paper 2083, 27 p.

Brooks, Rebekah, Clarke, J. S., and Faye, R. E., 1985, Hydrogeology of the Gordon aquifer system of east-central Georgia: Georgia Geologic Survey Information Circular 75, 41 p.

Buie, B. F., Hetrick, J. H., Patterson, S. H., and Neeley, C. L., 1979, Geology and industrial mineral resources of the Macon-Gordon kaolin district, Georgia: U.S. Geological Survey Open-File Report 79-526, 36 p.

Cahill, J. M., 1982, Hydrology of the low-level radioactive-solid-waste burial site and vicinity near Barnwell, South Carolina: U.S. Geological Survey Open-File Report 82-863, 101 p.

Callahan, J. T., 1964, The yield of sedimentary aquifers of the Coastal Plain southeast river basins: U.S. Geological Survey Water-Supply Paper 1669, 56 p.

Carlston, W. C., 1963, Drainage density and streamflow: U.S. Geological Survey Professional Paper 422-C, 8 p.

Carter, R. F., 1959, Drainage area data for Georgia streams: Unnumbered U.S. Geological Survey Open-File Report, 252 p.

----- 1983, Storage requirements for Georgia streams: U.S. Geological Survey Water-Resources Investigations 82-557, 65 p.

Carter, R. F., and Stiles, H. R., 1983, Average annual rainfall and runoff in Georgia, 1941-70: Georgia Geologic Survey Hydrologic Atlas 9, 2 sheets.

Christl, R. J., 1964, Storage of radioactive wastes in basement rock beneath the Savannah River Plant: E. I. DuPont De Nemours and Co. report DP-844, 105 p.

Clarke, J. S., Faye, R. E., and Brooks, Rebekah, 1983, Hydrogeology of the Providence aquifer of southwest Georgia: Georgia Geologic Survey Hydrologic Atlas 11, 5 sheets.

----- 1984, Hydrogeology of the Clayton aquifer of southwest Georgia: Georgia Geologic Survey Hydrologic Atlas 13, 6 sheets.

Clarke, J. S., Brooks, Rebekah, and Faye, R. E., 1985, Hydrogeology of the Dublin and Midville aquifer systems of east-central Georgia: Georgia Geologic Survey Information Circular 74, 62 p.

Cofer, H. E., and Manker, J. P., 1983, Geology and resources of the Andersonville, Georgia Kaolin and Bauxite District: U.S. Geological Survey Open-File Report 83-580, 95 p.

Cressler, C. W., Thurmond, C. J., and Hester, W. G., 1983, Ground water in the Greater Atlanta Region: Georgia Geologic Survey Information Circular 63, 144 p.

Daniel, J. F., 1976, Estimating ground-water evapotranspiration from streamflow records: Water Resources Research, v. 12, no. 3, p. 360-364.

Dingman, S. L., 1978, Drainage density and streamflow, a closer look: Water Resources Research, v. 14, no. 6, p. 1183-1187.

Eargle, D. H., 1955, Stratigraphy of the outcropping Cretaceous rocks in Georgia: U.S. Geological Survey Bulletin 1014, 101 p.

Faye, R. E., and Prowell, D. C., 1982, Effects of Late Cretaceous and Cenozoic faulting on the geology and hydrology of the Coastal Plain near the Savannah River, Georgia and South Carolina: U.S. Geological Survey Open-File Report 82-156, 73 p.

Faye, R. E., Carey, W. P., Stamer, J. K., and Kleckner, R. L., 1980, Erosion, sediment discharge, and channel morphology in the upper Chattahoochee River basin, Georgia: U.S. Geological Survey Professional Paper 1107, 85 p.

Faye, R. E., and McFadden, K. W., 1986, Hydraulic characteristics of Upper Cretaceous and Lower Tertiary clastic aquifers--eastern Alabama, Georgia, and western South Carolina: U.S. Geological Survey Water-Resources Investigations Report 86-4210, 22 p.

Fenneman, N. M., 1938, Physiography of eastern United States: New York, McGraw-Hill 714 p.

Fetter, C. W., 1980, Applied hydrogeology: Columbus, Ohio, Charles E. Merrill Publishing Company, 488 p.

Freeze, R. A., 1966, Theoretical analysis of regional groundwater flow: University of California at Berkeley, unpublished PhD thesis, 304 p.

Freeze, R. A., and Witherspoon, P. A., 1966, Theoretical analysis of regional groundwater flow: 1. Analytical and numerical solutions to the mathematical model: Water Resources Research, v. 2, no. 4, p. 641-656.

----- 1967, Theoretical analysis of regional groundwater flow: 2. Effect of water-table configuration and subsurface permeability variation: Water Resources Research, v. 3, no. 2, p. 623-634.

Georgia Department of Natural Resources, 1976, Geologic map of Georgia.

Glover, R. E., 1964, Ground-water movement: U.S. Bureau of Reclamation Engineering Monogram, no. 31, 76 p.

Hack, J. T., 1982, Physiographic divisions and differential uplift in the Piedmont and Blue Ridge: U.S. Geological Survey Professional Paper 1265, 49 p.

Harper, R. M., 1930, The natural resources of Georgia: University of Georgia, School of Commerce, Bureau of Business Research Study no. 2, Bulletin 30, 105 p.

Harr, M. E., 1962, Groundwater and seepage: New York, McGraw-Hill, 315 p.

Heath, R. C., 1983, Basic ground-water hydrology: U.S. Geological Survey Water-Supply Paper 2220, 84 p.

Hewett, D. F., and Crickmay, G. W., 1937, The warm springs of Georgia, their geologic relations and origins: U.S. Geological Survey Water-Supply Paper 819, 40 p.

Higgins, M. W., Atkins, R. L., Crawford, T. J., Crawford, R. F., III, and Cook, R. B., 1984, A brief excursion through two thrust stacks that comprise most of the crystalline terrane of Georgia and Alabama: Georgia Geological Society, Guidebook, 9th Annual Field Trip, 67 p.

Hitchon, Brian, 1969, Fluid flow in the western Canada sedimentary basin: Water Resources Research, v. 5, no. 1, p. 186-195.

Hubbert, M. K., 1940, The theory of ground-water motion: The Journal of geology, v. 48, no. 8, p. 785-944.

Ingersoll, L. R., Zobel, O. J., and Ingersoll, A. C., 1948, Heat conduction with engineering and geological applications: New York, McGraw Hill, 278 p.

Johnson, A. I., 1981, Glossary, in Permeability and ground water contaminant transport: American Society for Testing and Materials, STP 746, p. 3-17.

Johnston, R. H., 1973, Hydrology of the Columbia (Pleistocene) deposits of Delaware: Delaware Geological Survey Bulletin 14, 78 p.

----- 1976, Relation of ground water to surface water in four small basins of the Delaware Coastal Plain: Delaware Geological Survey Report of Investigation No. 24, 55 p.

----- 1977, Digital model of the unconfined aquifer in central and southeastern Delaware: Delaware Geological Survey Bulletin 15, 47 p.

LaMoreaux, P.E., 1946, Geology and ground-water resources of the Coastal Plain of east-central Georgia: Georgia Geological Survey Bulletin 52, 173 p.

Lee, R. W., 1984, Ground-water quality data from the southeastern Coastal Plain, Mississippi, Alabama, Georgia, South Carolina, and North Carolina: U.S. Geological Survey Open-File Report 84-237, 20 p.

LeGrand, H. E., 1962, Geology and ground-water resources of the Macon area, Georgia: Georgia Geological Survey Bulletin 72, 68 p.

LeGrand, H.E. and Furcron, A.S., 1956, Geology and ground-water resources of central-east Georgia: Georgia Geological Survey Bulletin 64, 174 p.

Leopold, L. B., Wolman, M. G., and Miller, J. P., 1964, Fluvial processes in geomorphology: San Francisco, W. H. Freeman, 522 p.

Linsley, R. K., Jr., Kohler, M. A., and Paulhus, J. L. H., 1975, Hydrology for engineers, Second Edition: New York, McGraw Hill, 482 p.

Lohman, S. W., 1972, Ground-water hydraulics: U.S. Geological Survey Professional Paper 708, 70 p.

Lohman, S. W., and others, 1972, Definitions of selected ground-water terms--revisions and conceptual refinements: U.S. Geological Survey Water-Supply Paper 1988, 21 p.

Marine, I. W., 1979, Hydrology of buried crystalline rocks at the Savannah River Plant near Aiken, South Carolina: U.S. Geological Survey Open-File Report 79-1544, 160 p.

McDonald, M. G., and Harbaugh, A. W., 1984, A modular finite-difference ground-water flow model: U.S. Geological Survey Open-File Report 83-875, 527 p.

Miller, J.A., 1986, Hydrogeologic framework of the Floridan aquifer system in Florida and parts of Georgia, Alabama, and South Carolina: U.S. Geological Survey Professional Paper 1403-B, 91 p.

Miller, J.A. and Renken, R.A., 1988, Nomenclature of regional hydrogeologic units of the Southeastern Coastal Plain aquifer system: U.S. Geological Survey Water-Resources Investigations Report 87-4202, 21 p.

Mitchell, G. D., 1981, Hydrogeologic data of the Dougherty Plain and adjacent areas, southwest Georgia: Georgia Geologic Survey Information Circular 58, 124 p.

Overstreet, W. C., and Bells, Henry, III, 1965, Geologic map of the crystalline rock of South Carolina: U.S. Geological Survey Miscellaneous Geological Investigations Map I-413, 1 sheet.

Poland, J. F., Lofgren, B. E., and Riley, F. S., 1972, Glossary of selected terms useful in studies of the mechanics of aquifer systems and land subsidence due to fluid withdrawal: U.S. Geological Survey Water-Supply Paper 2025, 9 p.

Prowell, D. C., Christopher, R. A., Edwards, L. E., Bybell, L. M., and Gill, H. E., 1985, Geologic section of the updip Coastal Plain from central Georgia to western South Carolina: U.S. Geological Survey Miscellaneous Field Studies Map MF-1737, 1 sheet.

Reinhardt, Juergen, Prowell, D. C., and Christopher, R. A., 1984, Evidence for Cenozoic tectonism in the southwest Georgia Piedmont: Geological Society of America Bulletin, v. 95, p. 1176-1187.

Renken, R. A., 1984, The hydrogeologic framework for the southeastern Coastal Plain aquifer system of the United States: U.S. Geological Survey Water Resources Investigations Report 84-4243, 26 p.

Riggs, H. C., 1963, The base-flow recession curve as an indicator of ground water: International Association of Scientific Hydrology Publication 63, p. 352-363.

Rorabaugh, M. I., 1960, Use of water levels in estimating aquifer constants in a finite aquifer: International Association of Scientific Hydrology Publication 52, p. 314-323.

----- 1964, Estimating changes in bank storage and ground-water contribution to streamflow: International Association of Scientific Hydrology Publication 63, p. 432-441.

Scott, J. C., 1962, Ground-water resources of Bullock County, Alabama: Geological Survey of Alabama Information Series 29, 120 p.

----- 1964, Ground-water resources of Russell County, Alabama-a reconnaissance: Geological Survey of Alabama Bulletin 75, 77 p.

Scott, J. C., Law, L. R., and Cobb, R. H., 1984, Hydrology of the Tertiary-Cretaceous aquifer system in the vicinity of Fort Rucker Aviation Center, Alabama: U.S. Geological Survey Water-Resources Investigations Report 84-4118, 221 p.

Siple, G. E., 1967, Geology and ground water of the Savannah River plant and vicinity, South Carolina: U.S. Geological Survey Water-Supply Paper 1841, 113 p.

South Carolina Water Resources Commission, 1983, South Carolina State Water Assessment-SCWRC Report No. 140, p. 10.

Stallings, J. S., and Peirce, L. B., 1957, Drainage area data for Alabama streams: Unnumbered U.S. Geological Survey Open-File Report, 103 p.

Stephenson, L. W., and Veatch, J. O., 1915, Underground waters of the Coastal Plain of Georgia: U.S. Geological Survey Water-Supply Paper 341, 539 p.

Stewart, J. W., 1964, Infiltration and permeability of weathered crystalline rocks, Georgia Nuclear Laboratory, Dawson County, Georgia: U.S. Geological Survey Bulletin 1133-D, 59 p.

Stewart, J. W., Callahan, J. T., and Carter, R. F., 1964, Geologic and hydrologic investigaiton at the site of the Georgia Nuclear Laboratory, Dawson County, Georgia: U.S. Geological Survey Bulletin 1133-F, 90 p.

Stokes, W. R., III, Hale, T. W., Pearman, J. L., and Buell, G. R., 1984, Water Resources Data for Georgia, 1983: U.S. Geological Survey Water-Data Report GA-83-1, 365 p.

Stricker, V. A., 1983, Baseflow of streams in the outcrop area of southeastern sand aquifer: South Carolina, Georgia, Alabama, and Mississippi: U.S. Geological Survey Water-Resources Investigations Report 83-4106, 17 p.

Thomson, M. T., and Carter, R. F., 1955, Surface water resources of Georgia during the drought of 1954: Georgia Department of Mines, Mining, and Geology Information Circular 17, 79 p.

Toth, Jozsef, 1962, A theory of ground-water motion in small drainage basins in central Alberta, Canada: Journal of Geophysical Research, v. 67, no. 11, p. 4375-4387.

----- 1963, A theoretical analysis of groundwater flow in small drainage basins: Journal of Geophysical Research, v. 68, no. 16, p. 4795-4812.

Toulmin, L. D., and LaMoreaux, P. E., 1963, Stratigraphy along the Chattahoochee River, connecting link between Atlantic and the Gulf Coastal Plains: American Association of Petroleum Geologists Bulletin, v. 47, no. 3, p. 385-404.

Trainer, F. W. and Watkins, F. A., 1975, Geohydrologic reconnaissance of the Upper Potomac River basin: U.S. Geological Survey Water Supply Paper 2035, 68 p.

U.S. Army Corps of Engineers, 1945a, Apalachicola River System, Chattahoochee River Profile: Mobile District, U.S. Army Corps of Engineers File No. 11-15-2-42.

----- 1945b, Apalachicola River System, Flint River Profile: Mobile District, U.S. Army Corps of Engineers File No. 11-15-8-41.

----- 1949a, Altamaha River Basin, Georgia Profile II: Savannah District, U.S. Army Corps of Engineers File No. DAS 301/3.

----- 1949b, Altamaha River Basin, Georgia Profile III: Savannah District, U.S. Army Corps of Engineers File No. DAS 301/4.

----- 1949c, Altamaha River Basin, Georgia Profile IV: Savannah District, U.S. Army Corps of Engineers File No. DAS 301/5.

----- 1949d, Altamaha River Basin, Georgia Profile V: Savannah District, U.S. Army Corps of Engineers File No. DAS 301/6.

----- 1959, Savannah River Stream Profile: Savannah District, U.S. Army Corps of Engineers File No. DSR 509.

----- 1965, Savannah River survey-Savannah River below Augusta, File No. DSR 100138: prepared by the Savannah District, U.S. Army Corps of Engineers.

----- 1972, Stream mileage tables with drainage areas, Mobile District, 165 p.

U.S. Geological Survey, 1975, Hydrologic unit map--1974, State of Georgia.

U.S. Study Commission--southeast river basins, 1963, Plan for development of the land and water resources of the southeast river basins--Hydrology, Appendix 10, 87 p.

Van Everdingen, R. O., 1963, Ground-water flow diagrams in sections with exaggerated vertical scale: Geological Survey of Canada, Paper 63-27, 102 p.

Vorhis, R. C., 1972, Geohydrology of Sumter, Dooly, Pulaski, Lee, Crisp, and Wilcox Counties, Georgia: U.S. Geological Survey Hydrologic Atlas HA-435.

Water Resources Data, Georgia, water year 1981: U.S. Geological Survey Water-Data Report GA-81-1, 446 p.

Winter, T. C., 1976, Numerical simulation analysis of the interaction of lakes and ground water: U.S. Geological Survey Professional Paper 1001, 45 p.

APPENDIX I
THE RORABAUGH - DANIEL METHOD OF HYDROGRAPH SEPARATION APPLIED TO REGIONAL DRAINS OF THE GEORGIA SUBREGION

This section describes the theory and application of the Rorabaugh-Daniel hydrograph separation technique, and includes an example of the methodology as applied to regional drain data of the Georgia Subregion.

Theory

The stream hydrograph can be regarded as an integral expression of the characteristics that govern the relations between rainfall, infiltration, evapotranspiration, and runoff for a particular watershed. The hydrograph reflects the two major contributions from the watershed, overland runoff and baseflow, as well as losses to the watershed such as pumping and evapotranspiration.

The discharge hydrograph typical of large rivers in the southeastern Piedmont and Coastal Plain is characterized by a sequential series of runoff and evapotranspiration occurrences which subdivide the hydrograph into several distinct intervals. During the initial part of the water year (October to December), stream discharge is typically low and annual low flows typically occur. Stream discharge characteristically rises following the onset of "killing frosts" and the reduction of evapotranspiration in late November or December. Throughout most of the winter and early spring, a series of weather fronts that produce rainfall generally cross the study area in relatively quick succession. The runoff generated by these storms initially causes stream discharge to rise rapidly and remain at a relatively high level through March or the early part of April. Following the cessation of winter rainfall and the onset of spring evapotranspiration, the hydrograph undergoes a period of recessions interrupted periodically by runoff generated by convective storms or hurricanes. A general recession characterizes the discharge hydrograph through the remainder of the water year. For the purposes of this report, the November-April period of relatively high and progressively increasing stream discharge is called the major rise period. The succeeding period of progressively decreasing streamflows and periodic runoff is termed the major recession period. Both periods are described analytically in this section and are labeled in figure 8.

All the methods used to separate stream discharge are to some degree subjective. The development and application of the Rorabaugh-Daniel method is, however, theoretically based, and results are consistent and generally reproducible. Part of the separation procedure is the computation of the ground-water contribution to evapotranspiration which is considered significant within the southeastern Coastal Plain.

Rorabaugh (1964) derived equation (4), which describes ground-water discharge to a stream following a uniform impulse of recharge by analogy to the heat flow equation of Ingersoll and others (1948),

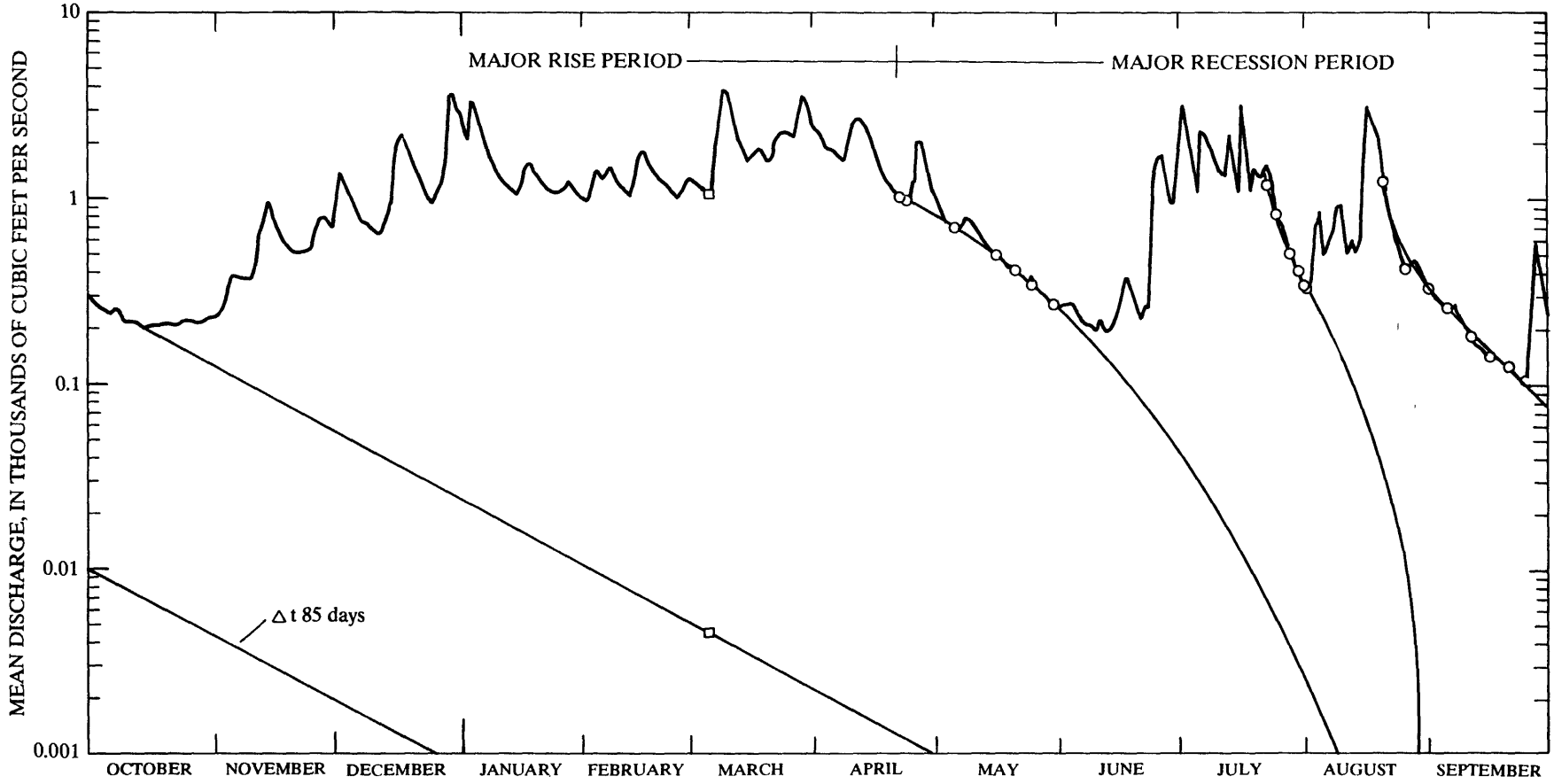

Figure 8.--Separation of the streamflow hydrograph of the Flint River near Culloden, Georgia, water year 1941.

$$q = 2T\ (h_0/a)\ (e^{-\pi^2 Tt/4a^2S} + e^{-9\pi^2 Tt/4a^2S} + e^{-25\pi^2 Tt/4a^2S} + ...), \quad (4)$$

where

q = ground-water discharge per unit of stream length, along one side of the stream (L^2T^{-1}),
T = aquifer transmissivity (L^2T^{-1}),
h_0 = instantaneous water-table rise (L),
a = distance from the stream to the ground-water divide (L),
t = time since water-table rise (T), and
S = aquifer storage coefficient (dimensionless).

Conditions assumed in the derivation of equation (4) are: the drainage basin is underlain by a uniformly shaped, homogeneous isotropic aquifer, distance from streams to ground-water divides are everywhere equal, the initial ground-water level is everywhere at stream level, and the aquifer is thick relative to h_0 and wide relative to its thickness.

Water-table fluctuations (h_0) in the study area probably do not exceed 30 ft/yr. For perennial streams in regional drain watersheds, h_0 is probably one to several orders of magnitude smaller than either aquifer widths (2a) or local ground-water flow lengths. Accordingly, where equation (4) is applied to streamflow recessions, one half the aquifer width (a) is considered equal to the average length of ground-water flow upstream from the gage.

Rorabaugh (1960, 1964) evaluated equation (4) for values of (Tt/a^2s) and determined that when Tt/a^2S exceeds 0.2 all but the first term of equation (4) become very small and may be neglected, yielding

$$q = 2T\ (h_0/a)e^{-\pi^2 Tt/4a^2S}. \quad (5)$$

Rorabaugh (1960, 1964) also demonstrated that when Tt/a^2S exceeds 0.2, a plot of the logarithm of discharge versus time becomes a straight line. The slope of the recession described by equation (5) after conversion to base 10 logarithms and plotted on semilog paper, equals

$$\text{slope} = 0.933a^2S/T. \quad (6)$$

Units of equation (6) are days per log cycle of discharge. The time required for Tt/a^2S to exceed 0.2 is termed the critical time (t_c) and can be shown as

$$t_c = 0.2\ a^2S/T. \quad (7)$$

Glover (1964) showed that at this time (t_c) one-half of the water from the recharge impulse has drained to the stream.

The determination of the straight-line recession slope is critical to the application of the Rorabaugh-Daniel hydrograph separation method. The slope is determined by inspecting the hydrograph for recessions during periods of little or no evapotranspiration (the major rise period). The chosen recessions should be long enough in time to extrapolate a straight-line trace across one log cycle of discharge. Once a slope is determined, it can be evaluated by using equations (6) and (7). From equation (6) a^2S/T can be determined and the critical time (t_c) can then be calculated using equation (7).

The critical time (t_c) is by definition the time required for the recession to become linear on semilog paper, and should approximate the time between an occurrence of high discharge and the following straight-line part of the recession. This procedure can be used as a self-check when inspecting hydrographs for representative recession limbs. The time required for the straight-line recession slope to decline one complete log cycle of discharge is defined as the streamflow-recession index (Bingham, 1982). In this report, streamflow-recession index is symbolized by Δt.

The experience of the writers indicates that for major drains in the southeastern Coastal Plain, at least 10 years of continuous streamflow record is required to evaluate the slope of the recession. The greater the period of record, the more accurate is the recession-slope determination.

In equation (4) the instantaneous water-table rise (h_0) can be described as a uniform increment of head resulting from a recharge impulse instantaneously applied to the aquifer and allowed to drain to the stream. To describe a constant rate of recharge, equation (4) is integrated for the condition $dh/dt = C$ such that,

$$q = CaS\,[1-(8/\pi^2)\,[e^{-\pi^2 T/4a^2 S} + (1/9)e^{-9\pi^2 Tt/4a^2 S} + (1/25)e^{-25\pi^2 Tt/4a^2 S}...]]. \quad (8)$$

Rorabaugh (1964) showed that when Tt/a^2S is larger than 2.5 all but the first term become inconsequential, yielding

$$q = CaS, \quad (9)$$

which describes steady-state-flow conditions.

Equation (8) defines the dimensionless plot shown in figure 9. The plot is a dimensionless type curve of the time-discharge relation during recharge at a constant rate, and is used to compute aquifer discharge (Rorabaugh, 1964).

The combination of equations (4) and (8), when dh/dt is positive, yields

$$q = (h_0T/a)(Ca^2S/h_0T)\,[\,1+2\sum_{m\,=\,1,\,2,\,5}^{\infty}(h_0T/Ca^2S - 4/\pi^2m^2)\,e^{-m^2\pi^2 Tt/4a^2S}]. \quad (10)$$

When dh/dt is negative, flow from the aquifer occurs other than as discharge to the stream, and the combination of equations (4) and (8) may be described by the family of dimensionless type curves shown in figure 10. This family of type curves is employed to determine aquifer discharge to evapotranspiration.

The use of these type curves (figs. 9 and 10) and related equations to separate streamflow hydrographs and to compute baseflow and ground-water contribution to evapotranspiration is demonstrated in the following section.

Application of Rorabaugh-Daniel Method

The U.S. Geological Survey operates a gaging station on the Flint River near Culloden (02347500, pl. 1) in west-central Georgia (pl. 3). The drainage area of the river at this station is approximately 1,850 mi^2 and the drainage pattern is predominately dendritic. No streamflow regulation exists within the

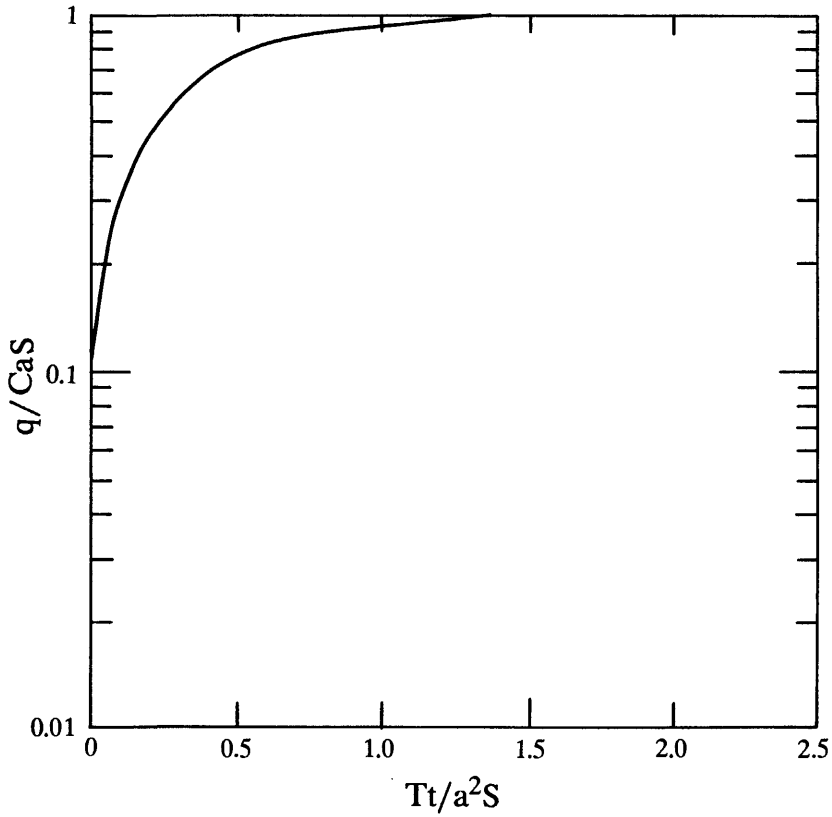

Figure 9.--Dimensionless type curve of time-discharge relation during a constant recharge rate. Modified from Rorabaugh, 1964.

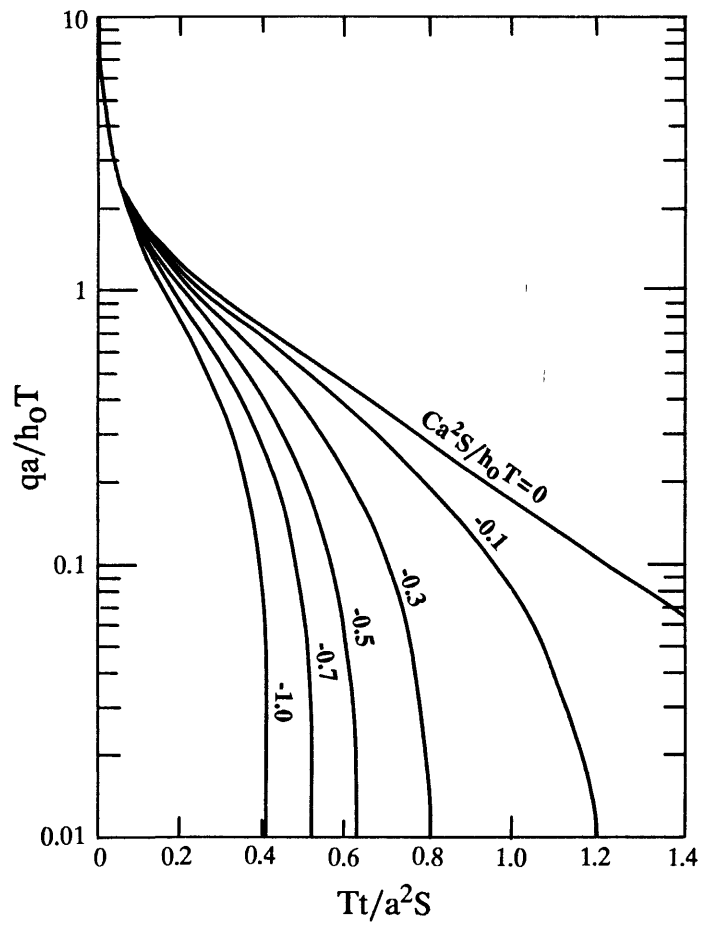

Figure 10.--Dimensionless type curves of streamflow resulting from sudden recharge to a leaky aquifer. From Daniel, 1976.

drainage basin and the streamflow records are considered to be good (Stokes and others, 1984). Average annual precipitation within the basin is about 50 in/yr (Carter and Stiles, 1983).

This part of the Flint River watershed is within the Piedmont Lowlands and is characterized by low relief, averaging about 50 m in a 100 km^2 area (Hack, 1982). The basin is underlain by typical Piedmont rocks in all but the southern margin, which contains the Macon melange (Higgins and others, 1984). Much of the rock within the basin is fractured and there are numerous minor faults.

Ground-water flow within the basin is thought to be primarily controlled by fractures in the bedrock. These secondary permeability features are common throughout the basin and many are associated with seeps and springs. Although there is only circumstantial evidence, it is postulated that some of the fractures reach significant depth (Hewett and Crickmany, 1937; M. W. Higgins, U.S. Geological Survey, oral commun., 1985). The regolith in the basin, which locally exceeds 150 ft in thickness, also contributes significantly to the ground-water flow to streams and regional drains.

More than 50 annual hydrographs representing average daily stream discharge of the Flint River near Culloden, Ga., were inspected for recessions during major rise periods. A streamflow-recession index of 85 days was identified. Thus, using equation (6), a^2S/T was determined to be 91 days (91 days = 85 days/0.933). The time required for the recession slope to become straight is therefore less than or equal to the critical time ($t_c = 0.2(a^2S/T)$, or approximately 18 days. Inspection of numerous hydrographs revealed that high discharge commonly occurred about 18 days prior to the straight-line part of a recession limb.

A single streamflow-recession index was noted repeatedly throughout the streamflow record. This index is inversely related to the hydraulic diffusivity (T/S) of the basin aquifers and represents the integrated effect of the entire range of values of aquifer transmissivity (T) and aquifer storativity (S) in the basin (Daniel, 1976). Although the watershed is not underlain by a homogeneous isotropic aquifer, the consistent recession index indicates that at the regional scale the ground-water-flow system responds as such, and may be considered monolithologic (Carlston, 1963).

Figure 8 shows the hydrograph for water-year 1941 and illustrates the application of the Rorabaugh-Daniel method. The major features of the hydrograph are the major rise period, which begins in mid-October and lasts through mid-April, and the major recession period which lasts from mid-April through September. The major rise period displays progressively increasing stream discharge, a significant part of which is ground-water discharge. Given the time of occurrence, the major rise period is considered to be a period of ground-water discharge to the stream that is exclusive of ground-water loss to evapotranspiration.

A slope representing the recession index was applied to the hydrograph on October 14, which is the day of the lowest daily discharge preceding the major rise period, and the time at which constant recharge to the aquifer was assumed to begin. Because evapotranspiration is low during much of the major rise period, aquifer discharge is determined by using equation (8) and the related type curves (fig. 9).

To determine the rate of aquifer discharge under steady-state conditions a value for Tt/a^2S that approaches 2.5 is desired. As noted earlier, when Tt/a^2S exceeds 2.5, steady-state conditions are attained and q = CaS. This condition is best satisfied late in the major rise period, where a large value of t would yield a large value for Tt/a^2S. March 5th was subjectively chosen because it corresponds to a low discharge that occurred near the end of the major rise period, 142 days after October 14th. Using a value of 142 days for t, a value for Tt/a^2S is computed to be 1.56 (step A, fig. 11). From the type curve of figure 16 a value of 1.56 for Tt/a^2S corresponds to a value of approximately 0.99 for q/CAS (step B, fig. 11). Aquifer discharge is computed by subtracting the respective recession index discharge value from total stream discharge and is approximately 1,050 ft^3/s. By substitution and algebraic solution (step C, fig. 11), the aquifer discharge rate represented by CAS equals about 1,060 ft^3/s. Areally, the computed constant aquifer-discharge rate during the major rise period equals 2.05×10^{-8} feet per second (ft/s), or 0.021 inches per day (in/day), or 4.02 inches (in.). Although computed from characteristics relative only to the major rise period, the total computed discharge of 4.02 in. represents total discharge from the aquifer within the drainage basin during the period October 14 through late June when significant discharge again occurs.

The recession following the major rise period occurs from mid-April through early June. For this period aquifer discharge to evapotranspiration was calculated using equation (10) and the related type curves (fig. 10). The hydrograph was replotted after subtraction of the October recession index discharge values. Values of discharge and corresponding Tt/a^2S for several days were calculated, tabulated, plotted (fig. 11), and compared with the type curves of figure 10 to determine the best fit for the entire recession period (step D, fig. 11). The comparison indicated a best average fit of Ca^2S/h_oT equal to -0.1 and Tt/a^2S equal to 1.19. From the same comparison a match point was chosen at qa/h_oT equal to 1.0 and Q equal to 1,450 ft^3/s (step E, fig. 11). Values for all the variables necessary for solution of aquifer discharge to evapotranspiration as represented by CAS are now available. Substitution and algebraic solution for CAS yields a value of 145 ft^3/s (step F, fig. 11). Areally, the computed constant aquifer-discharge rate to evapotranspiration, CS, during the period mid-April through early June equals 2.8×10^{-9} ft/s, or 2.9×10^{-3} in/day, or 0.32 in. (step F, fig. 11). The length of the recession period is found by multiplying Tt/a^2S by a^2S/T as shown in step F of figure 11.

The major recession period displays a series of peaks in July and August that are typical of summer convective-storm activity. These two occurrences of increasing discharge were separated to determine both total aquifer discharge and aquifer discharge to evapotranspiration. Aquifer discharge to evapotranspiration for the July event was calculated by using equation (10) and the related type curves (fig. 10). The recession at the end of July was replotted after subtraction of the April-May recession discharge values. Values of discharge and corresponding Tt/a^2S for several days were calculated, tabulated, plotted, and compared with the type curves of figure 10 (step A, fig. 12). The best fit indicated Ca^2S/h_oT equal to 1.0, and Tt/a^2S equal to 0.41. The match point was chosen at qa/h_ot equal to 1.0 and Q equal to 300 ft^3/s. Substitution and algebraic solution for aquifer discharge to evapotranspiration as represented by CAS equals 300 ft^3/s (step B, fig. 12). Areally, the computed aquifer-discharge rate to evapotranspiration, CS, following the July storm equals 5.8×10^{-9} ft/s, or 0.006 in/day, or 0.22 in. for the recession period (step C, fig. 12).

Calculation of aquifer discharge during major rise period of figure 8

$t_2 - t_1$ = streamflow recession index = 0.933 a^2S/T = 85 days
A = 1850 mi.^{2} a^2S/T = 91 days

STEP A

Period of October 14 through March 5 equals 142 days; t = 142 days, therefore $t/(a^2S/T) = 1.56$

STEP B

From figure 9, for $Tt/a^2S = 1.56$, $q/CaS = 0.99$

STEP C

Discharge on March 5 minus recession value = Q = (1050 - 4) = 1046 ft^3/s

L = total stream length, A = a2L = drainage area (Daniel, 1976)

Q = q2L (Daniel, 1976)

q/CaS = Q/2L (2L/CAS) = Q/CAS, therefore CAS = Q/(q/CaS)

CAS = Q/(q/CaS) = (1046 ft^3/s)/0.99 = 1057 ft^3/s

CS, constant rate of discharge areally = Q/(q/CaS) A

CS = Q/(q/CaS) A = (1046 ft^3/s)/(0.99)(1850 mi.^{2}) = 2.05 x 10^{-8} ft/s

Major rise period, (October 14 -- April 21) = 189 days

Calculation of aquifer discharge to evapotranspiration during recession following major rise period.

STEP D

Date	t (d)	Discharge (ft^3/s)	Tt/a^2S
April 21	1	1028	0.011
April 23	3	968	.033
May 5	14	673	.154
May 15	24	520	.264
May 20	29	412	.319
May 23	32	362	.352
May 30	39	267	.429

STEP F

$$CAS = \frac{(Ca^2S/h_oT)(Q)}{qa/h_oT}$$

$$CAS = \frac{(0.1)\ 1450\ ft^3/s}{1.0} = 145\ ft^3/s$$

$$CS = \frac{(Ca^2S/h_oT)\ (Q)}{(qa/h_oT)(A)} = 2.8 \times 10^{-9}\ ft/s$$

Recession period = $(Tt/a^2S)(a^2S/T)$ =

(1.19)(91days) = 108 days

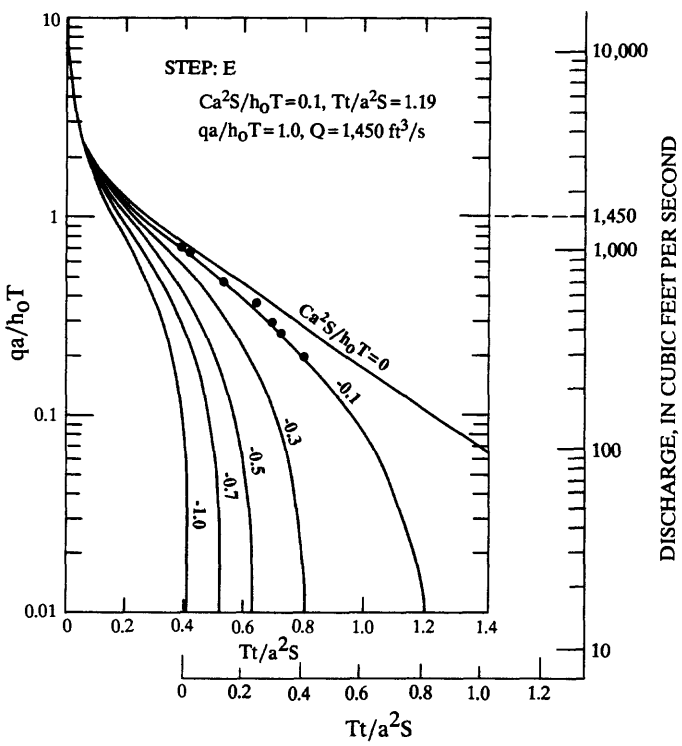

Figure 11.-- Calculation of aquifer discharge during the major rise period and calculation of aquifer discharge to evapotranspiration during the subsequent recession - Flint River near Culloden, Georgia - water year 1941

Calculation of aquifer discharge to evapotranspiration

STEP A

Date	t (d)	Discharge (ft^3/s)	Tt/a^2S
July 22	1	1548	0.011
July 24	3	934	.033
July 27	6	582	.066
July 29	8	452	.088
July 31	10	391	.110
August 1	11	356	.121

STEP B

$$CAS = \frac{(Ca^2S/h_oT)\,Q}{qa/h_oT}$$

$$CAS = \frac{(1.0)\ 300\ ft^3/s}{1.0} = 300\ ft^3/s$$

STEP C

$$CS = \frac{(Ca^2S/h_oT)\,Q}{(qa/h_oT)\,A} = 5.8 \times 10^{-9}\ ft/s$$

Recession period = $(Tt/a^2S)(a^2S/T)$ =

(0.41)(91 days) = 37 days

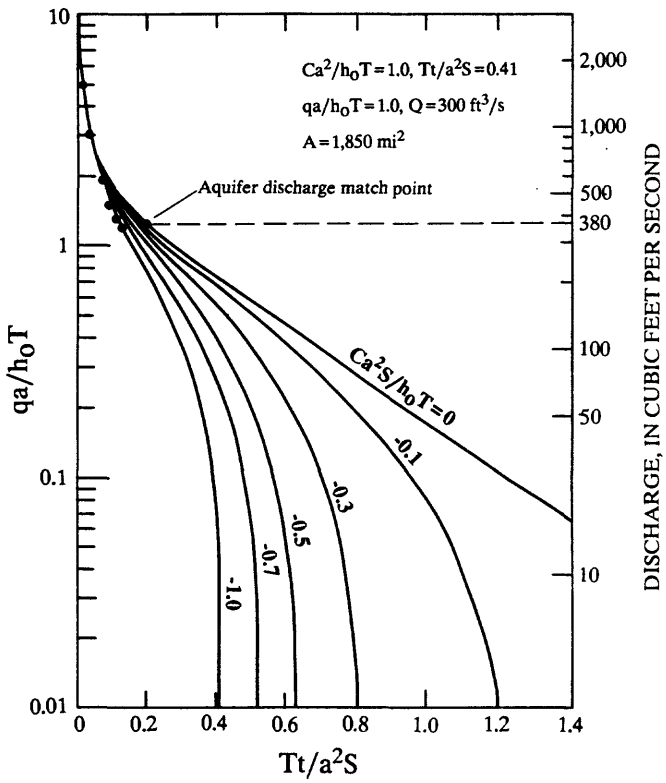

Calculation of total aquifer discharge

For match point $Ca^2S/h_oT = 0.0$, $Tt/a^2S = 0.2$, discharge (Q) = 380 ft^3/s

$V = 2Q\ (0.405\ a^2S/T)$

$V = 2\ (380\ ft^3/s)(0.405)(91\ days) = 2.43 \times 10^9\ ft^3$

recession period = 37 days, aquifer discharge = 760 ft^3/s

Areally, aquifer discharge = 1.47×10^{-8} ft/s

Figure 12.-- Calculation of total aquifer discharge and aquifer discharge to evapotranspiration during the July recharge occurence of the major recession period - Flint River near Culloden, Georgia, July 1941

Total aquifer discharge during the July storm event was calculated volumetrically using a simplified form of equation (5) and is shown in figure 12. Rorabaugh (1964) integrated equation (5) with respect to time (t) to obtain the volume of water discharged, which under steady-state conditions equals the volume of the recharge impulse, as

$$V = q(4a^2S/\pi^2T). \quad (11)$$

A conversion to base 10 logarithms and doubling to represent total recharge from both sides of the stream yields

$$V = 2q(0.933a^2S/T). \quad (12)$$

A value of a^2S/T is known (91 days), and the remaining variable, q, is determined using the type curves of figure 10. From the type curves of figure 10, a match point of Ca^2S/h_0t equal to 0.0, and Tt/a^2S equal to 0.2 describes a discharge, (Q) of 380 ft^3/s. Substitution and algebraic solution for volumetric ground-water recharge gives V equal to 2.43×10^9 ft^3. Assuming a constant rate for the 37-day period, aquifer discharge rate equals 760 ft^3/s. Areally, total aquifer discharge during the July storm, and hence the corresponding rate of recharge equals 1.47×10^{-8} ft/s, or 1.52×10^{-2} in/d, or 0.56 in.

The high discharge occurrence in mid-August (fig. 8) was separated in the same manner as the July event. Total aquifer discharge was computed to be 0.44 in., and aquifer discharge to evapotranspiration was computed to be 0.11 in.

The results of the hydrograph separation are presented in table 19. Aquifer discharges for the major rise period, and the two rise events of the major recession period were totaled to determine total annual aquifer discharge. Aquifer discharges to evapotranspiration for the major recession period were totaled to determine total annual aquifer discharge to evapotranspiration. Annual aquifer discharge to the stream, computed as the difference between total annual aquifer discharge and annual aquifer discharge to evapotranspiration, was determined to be approximately 4.4 in. areally, or 600 ft^3/s (table 19). Under the idealized and near steady-state conditions described by the solution procedure, the aquifer discharge to the stream represents at least a minimum value of the recharge to the aquifer.

Qualifications and Limitations

Several major assumptions and simplications regarding basin boundary conditions, aquifer characteristics, and variations in recharge and evapotranspiration were applied to the theoretical development and use of the Rorabaugh-Daniel hydrograph separation method. The two major assumptions regarding the geometry and boundary conditions of the basin are (1) the ground-water flow distance a is everywhere equal within the drainage basin and (2) ground-water and surface-water divides are coincident. Both of these assumptions are dependent on the scale of the application. The value a for this study is considered the average length of ground-water flow within the watershed area contributing to a stream reach. An effective length is said to exist for the watershed area which produces the observed recession characteristics. Where this effective length is not generally constant, a variety of recession characteristics would probably occur at the stream station and the method of analyses described in this paper would not be applicable. Note that the value a is not needed to determine aquifer discharge.

Table 19.--Summary of aquifer discharges computed by hydrograph separation for the Flint River near Culloden, Georgia--water year 1941

Aquifer discharge	Inches
October-May	4.02
June-July	.56
August-September	.44
Annual total	5.02
Aquifer discharge to evapotranspiration	**Inches**
April-June	0.32
July	.22
August-September	.11
Annual total	0.65
Annual aquifer discharge to the stream	**Inches**
	5.02
	- .65
	4.37

The correspondence between topographic and hydrologic boundaries in the study area has been previously established in conjunction with descriptions of the conceptual model and transverse flow to cross-section model path lines. Potentiometric maps shown in Faye and Prowell (1982), Clark and others (1983, 1984, 1985), and Brooks and others (1985) indicate a high degree of correspondence between surface drainage characteristics and aquifer boundaries within the northern part of the Georgia Subregion.

The assumption that aquifer characteristics are isotropic and homogeneous throughout the basin is fundamental to the development and application of the Rorabaugh-Daniel method. This assumption would seem to limit this method to smaller ground-water drainages, or at least to simplistic drainages. It is important to realize that the streamflow-recession index represents the integrated effect of the diffusivity (T/S) of the entire drainage. If a consistent and reproducible streamflow-recession index is identified using a long period of record, it may be taken as an indication that the contributing aquifer responds effectively as an isotropic, homogeneous porous medium with a

constant diffusivity at the represented scale, regardless of geologic or lithologic variability. Conversely, when a consistent recession index cannot be identified, it may be suspected that aquifer characteristics are effectively heterogeneous throughout the contributing area. The occurrence of multiple-recession indices might indicate multiple aquifers with significantly different hydraulic characteristics.

In general, more than 20 years and at least 10 years of unregulated streamflow record at each regional drain gage was used to evaluate each reported streamflow-recession index (table 12). Consistent and reproducible streamflow-recession indices were identified at all but one station, the Savannah River at Burtons Ferry Bridge.

Daniel (1976) presents a thorough discussion of the assumptions regarding the computation of recharge and evapotranspiration. The most important assumptions are (1) that recharge occurs as an impulse occasioned by a uniform water-level increase throughout the basin and (2) that aquifer discharge to evapotranspiration occurs at an equal and constant rate throughout the period, throughout the watershed. Although field conditions rarely, if ever, exactly correspond to these assumptions, the observed response of ground-water levels and related streamflows in the study area (Clarke and others, 1985, figs. 6, 7, and 8A) during the major rise and recession periods generally indicates a relatively short period of rapid recharge to aquifers followed by an extended period of uniform, relatively constant aquifer discharge (evapotranspiration and baseflow). Daniel (1976) points out that the values of recharge and evapotranspiration are considered to be components of an idealized system with different dimensions but with flow characteristics identical to the ground-water drainage being investigated.